Comments to the Author:
Dear Authors
Thank-you for your much-revised manuscript. I intend to send it back to the two referees who were willing to review a revised manuscript. However, I have many detailed comments of my own (see below), generally intended to make it clearer for the reader. I think these are best attended to before the referees review it.
Yours sincerely
John Huthnance (editor)

Page 1
Line 2. “then completed” -> “complemented”?
Answer: Corrected

Line 10. “which” -> “as” (only use “which” immediately after the object it refers to)
Answer: Corrected

Line 11. Omit “that it offers”
Answer: Corrected

Line 17. “should be considered with attention” -> “merits attention”?
Answer: Corrected

Lines 19-20. “a decrease in freshwater content of about 180km^3” – from when to when?
Answer: Over 2003-2014 period

Page 2
Line 2. “500 km^3” – over what time period? Are these freshwater volumes on the basis of salinity = 0?
Answer:
500 km^3 is the volume of exchange between the Laptev and the East-Siberian Seas and central Arctic ocean with anticyclonic atmospheric vorticity conditions, it was calculated from 1920-2005 hydrographic measurements on “quasi-decadal timescales” based on the estimates of freshwater content anomaly and thus, mean salinity values

Lines 3-4. “income in” -> “coming into”
Answer: Corrected

Lines 8-9. “The shelf area of the Laptev and the East-Siberian was described” -> “The Laptev Sea and East-Siberian shelf areas were described”
Answer: Corrected

Line 10. “the freshwater income” -> “the incoming freshwater”
Answer: Corrected

Line 21. “falls under an additional impact” -> “comes under the additional influence”
Answer: Corrected

Line 29. “via” needs to be replaced by some characteristic of the vertical distribution of energy that shows the extent of the mixed layer.
Answer:

The note on the energy was excluded as I do not remember the details, and the book where it comes from has only a paper version and is situated in another country now, so unavailable with coronavirus situation.

Lines 30-31. “open water or under the ice, the Barents Sea, the East-Siberian Sea or the central Arctic”; this list is only useful if you associate different MLD with each region.
Answer:
Added details on the region and time of measurement for all citations

Page 3
Line 7. “water, which” -> “water; 34.80”
Answer: Corrected

Line 10. “being” -> “to be”
Answer: Corrected

Line 15. “layer between” -> “layer to be between” or “layer as between”
Answer: Corrected

Line 18. Omit “The” at start.
Answer: Corrected

Line 29. Omit first “the”.
Answer: Corrected

Line 33. “and” -> “over a”?
Answer: Corrected

Page 4
Line 1. “net radiative balance at the sea surface changes from 100W/m^2” – in which direction is the 100W/m^2 ?
Answer: Positive values mean from the atmosphere to the ocean and correspond to the warming of sea water in summer

Lines 3-12. This is the place (end of Introduction) to state clearly what your paper will do to improve our knowledge and understanding. That statement is rather hidden by, and mixed up with, too much information about how you will do it. Such information can be in section 2.
Answer:
Thank you for your suggestions! We moved the line 8-12 to the second section, Data and methods.

Line 18. Omit “both,”
Answer: Corrected

Page 5 line 6. Omit “further on”?
Answer: Corrected

Page 6 line 4. “The threshold chosen for practical density gradient was 0.3 degree per 1 m” does not read sensibly. “0.3 degree per 1 m” relates to temperature (your text says so) so how does the density relate to the threshold?
Answer: It is a typo, thank you. 0.3 relates to density, corrected the units to kg/m^3 per 1 m.

Page 6 bottom – page 7 top. “the upper 12 m of the surface layer was homogeneous, and our CTD and TSG measurements can be used for the validation of satellite data." I think 12m homogeneous layer validates the TSG at 6.5m (a referee question) but the satellite data may have a skin effect and/or diurnal variation depending on the weather (you discuss this on pages 9-10).

Answer: These effects are supposed to be filtered out when a product L4 is proposed. We can still confront some non-filtered effects, indeed.

Page 7
Line 3. ". . Below 40m depth the temperature . .". It may be better to give the temperature at 30m depth; at present you describe the temperature as "0.5◦C . . at 5 m . . slightly rising to -1 ◦C"

Answer:
I suppose that "40 m" in this question might be a typo. 40 m is the depth of the smallest STD of temperature. Added to the text the following precision:
We observe rather cold (0.5° C) and fresh (30.5) water at 5 m, followed by a smooth thermo- and halocline down to 30 m depth (with a temperature of -1.3° C and salinity of 33.8)

Line 5. Omit "up"
Answer: Corrected

Line 20. "Since" -> "After"
Answer: Corrected

Line 23. "Siberian great" -> "large Siberian"
Answer: Corrected

Line 25. "moment" -> "time".
Answer: Corrected

Line 29. "listed below products" -> "products listed below"
Answer: Corrected

Page 8
Line 4. "provide" -> "providing"
Answer: Corrected

Line 7. "uses" -> "used"
Answer: Corrected

Lines 18 and 19. "collocated" or "co-located"? I think maybe "collocated" in line 18 (also line 21 and page 9 line 2) but "co-located" in line 19.
It is not clear to me that you "collocated" SST DMI (line 19 and figure 4 caption).
Answer:
Corrected to co-located in line 19 and figure 4 caption.
We meant a stage in data processing when the closest pixel of SST (or SSS) image is found for every in situ measurement of chosen coordinates and date.

Page 10
Line 25. "embarking" -> "carrying"?
Answer: Corrected

Line 32 to page 11 top line. This sentence is hard to read. You might move all the definitions / explanations to the end.
Answer: Corrected to following:
"To create SST DMI L4 product, only the observations between 21:00 and 7:00 local time are used (\citet{hoyer2014bias}), thus, local diurnal variations of SST are supposed to be filtered out. Diurnal variation of temperature might be present in real in situ measurements in case of strong diurnal warming events, but no particular observations allowing to investigate this question were done during the cruise."

Page 11.
Line 4. "at attempting to retrieve" -> "at retrieving". ["aims . . at attempting" is duplication.]
Answer: Corrected

Line 16. "weighted by the estimated error" suggests more weight is given to values with larger estimated error. Maybe "weighted by comparison with the estimated error" or "weighted relative to the estimated error"?
Answer: Corrected to "weighted relative to the estimated error"

Lines 21, 22. I missed definition of "ACARD" that would give meaning to a value 45. Perhaps a reference would be best.
Answer: "Waldteufel, P., Vergely, J. L., Cot, C., "A modified cardioid model for processing multiangular radiometric observations," IEEE Transactions on Geoscience and Remote Sensing, vol. 42, pp. 1059-1063, 2004."

Line 32 and figure 5 caption. I am not sure about "collocated SSS" (c.f. Page 8 comment above).
Answer: Corrected to co-located

Page 13
Lines 4-5. "a higher confidence" -> "confidence"? ["higher" implies comparison – with what?]
Answer: Corrected

Line 15. "polynya" (spelling)
Answer: Corrected

Line 16. "south of 79◦N" (assuming you mean that it was ice-free at 78◦N, for example).
Answer: Corrected

Page 14.
Equations (1). For Ekman transports I think you should not divide by Ekman depth. The division gives a velocity. Also I think your w_ekm has the wrong dimensions.

Answer:
Thank you for correction. Indeed, we had a velocity instead of horisontal transport in the Equation 1 (corrected the formulae to a version without division by Ekman depth, thus using [m^2/s]). As for the vertical Ekman velocity, which is given in [cm/s], the derivation of this equation is well demonstrated in http://www.geo.cornell.edu/ocean/p_ocean/ppt_notes/16_EkmanTransport.pdf, page 6.

Line 28. I think "freshwater" -> "water" twice (you give the salinity values anyway and it is not actually "fresh"; maybe "fresher"?).
Answer :

Corrected to “Water with salinity … . Additional fresher water from the Kara Sea…”

Page 15.
Figure 6b black line needs explanation.
Answer : Added “The dotted lines in Figure (b) show the position of sea ice edge at different moments of time before and during the ARKTIKA-2018 cruise”

Line 7. “sensibility” -> “sensitivity”?
Answer: Corrected

Page 17 line 3. Omit “back” or replace with a word giving extra meaning.
Answer: Corrected

Page 18
Table 1 caption. “ans” -> “and”; “explication” -> “explanation”
Answer: Corrected

Line 18. “in a previous section” is too vague; give the section number.
Answer: Corrected

Page 19 Figure 8. I do not see the red freezing line mentioned in the caption.
Answer : At the bottom of every figure in this panel a thin red line shows the freezing temperature for different salinity.

Page 21
Figure 10 caption line 2. Better “Small coloured circles”.
Answer: Corrected

Line 3. Omit “,”
Answer: Corrected

Page 23
Figure 12. I rather agree with referee 1 that these Hovmoeller plots would be better with time as the “y” axis and (increasing) latitude as the “x” axis.
Answer:
Thank you for your suggestion. We discussed this question with co-authors and agreed to keep the same form as presented. There is “geographical” meaning in the presentation with x-axes for time and y-axis for latitude, and we would prefer to show it this way.

Lines 2-4. I think referee 2 had questions about wind direction and mixing. Your point about an error in DMI SST avoids the need to answer those questions but it is not clear why “an error in DMI SST product” should be “due to . . strong winds”

Answer : The error in SST-retrieval are related to the cloud masking and a special correction for the “skin temperature” to bring it to subskin values. This correction is usually uniform for the whole basin and is calculated for the low-wind speed conditions (e.g. 0.17 Kelvin for the Arctic Ocean, see Hoyer et al. 2014, p.203)

Hoyer, J. L., Le Borgne, P., and Eastwood, S. (2014). A bias correction method for arctic satellite sea surface temperature observations. Remote Sensing of Envi- ronment, 146:201–213.

Line 3. Omit “on”.
Answer: Corrected

Line 7. “depression” -> “cyclone”?
Answer: Corrected

Page 24
Line 1. Please explain what “frontal area” you refer to.
Answer:
We mean the surface thermal and salinity fronts, marked as the sharpest gradients.

Lines 4-5. “Higher values . . are expected . . as this is an area exposed to rapid changes.” Please explain.
Answer:
As the timeseries of SST and SSS fields is short, the easiest way to see any variability is to observe the area with dramatic changes of SST or SSS (frontal area). This rapid and explicit variability of oceanic characteristics (SST and SSS) could be related to the rapid (usually more rapid by its nature) atmospheric variability in the wind speed or sea level pressure.
We excluded this sentence to avoid confusion.

Page 25
Lines 13-14. “presented below oceanographic sections” -> “oceanographic sections presented below”
Answer: Corrected

Lines 19-20. Move “(20-30m)” to after “similar” in line 19.
Answer: Corrected

Line 21. “which is clearly seen in temperature signal” -> “as is clearly seen in the temperature”
Answer: Corrected

Line 25. “deepens” -> “moves deeper”
Answer: Corrected

Page 26 line 10. “first (surface)” -> “surface”?
Answer: Corrected

Page 27.
Line 4. “sea edge very slowly” looks like a mistake. Or it needs explaining!
Answer:
Corrected to “It is interesting that the areas with the highest sea ice melt fraction (Fig.\ref{fig: dO18}, c) (5-10%) very slowly follow the sea edge, so they were observed in the central and western part of the Laptev sea and in the MIZ area in the East-Siberian Sea.”

Line 12. “In a previous study on” -> “A previous study in”
Answer: Corrected

Page 28
Lines 3-4. “The cross-validation of satellite DMI SST and SMOS SSS "A" estimates is done with rare in this region continuous TSG measurements and CTD data. “ I think you want “Satellite DMI SST and SMOS SSS "A" estimates are cross-validated with continuous TSG measurements and

CTD data (rarely done in this region)."
Answer: Corrected

Line 8. ". . and to discuss . ."
Answer: Corrected

Line 12. I don't understand "and diminishes"
Answer: Deleted "diminishes"

Line 14. "which" -> "as"
Answer: Corrected

Page 29
Line 3. "is to start in" -> "starts at"?
Answer: Corrected

Line 4. "will be finished by November"? The surface may be completely covered by ice but surely the ice will continue forming under the surface through the winter?
Answer: Yes, definitely. We meant that the sea surface will be covered by ice.

Lines 18-19. "Ekman depth is controlled only by the Coriolis parameter f"? Also by viscosity!
Answer:
Indeed, thank you for reminding. Added to the text.

Page 30
Line 30. "precised" -> "stated"? "Rossby" (spelling)
Answer: Corrected

Line 31. "altimeter along-track resolution of 300 m" seems very fine. Some km "footprint"?
Answer:
Corrected to the "altimeter along-track sampling of 300 m", as it is mentioned in Armitage et al., 2017, p.1773. Indeed, 300 m is the distance between two succeeding measurements, while the "footprint" of, e.g. Sentinel-3 altimeter in Low Resolution Mode is 1.64 km.

Lines 31-32. "at the shallowest areas the highest eddy kinetic energy was reported in the same study." -> "the same study reported largest eddy kinetic energy in the shallowest areas"?
Answer: Corrected

Page 31 line 4. "thank for" – thank who?
Answer: Thank you for your remark, it was a mistake, the "isotopes analysis" acknowledgements are given below.

Surface waters properties Properties of surface water masses in the Laptev and the East-Siberian Seas in summer 2018 from in situ and satellite data

Anastasiia Tarasenko[1, 2], Alexandre Supply[3], Nikita Kusse-Tiuz[1], Vladimir Ivanov[1], Mikhail Makhotin[1], Jean Tournadre[2], Bertrand Chapron[2], Jacqueline Boutin[3], Nicolas Kolodziejczyk[2], and Gilles Reverdin[3]

[1]Arctic and Antarctic Research Institute, Saint-Petersburg, Russia
[2]Univ. Brest, CNRS, IRD, Ifremer, Laboratoire d'Océanographie Physique et Spatiale (LOPS), IUEM, Brest 29280, France
[3]Sorbonne Université, CNRS, IRD, MNHN, Laboratoire d'Océanographie et du Climat, Expérimentations et Approches Numériques (LOCEAN), Paris, France

Correspondence: Anastasiia Tarasenko (tad.ocean@gmail.com)

Abstract. Variability of surface water masses of the Laptev and the East-Siberian seas Seas in August-September 2018 is studied using in situ and satellite data. In situ data was were collected during ARKTIKA-2018 expedition and then completed with satellite estimates of complemented with satellite-derived sea surface temperature (SST) and salinity (SSS), sea surface height, satellite-derived wind speeds and sea ice concentrations. Derivation of SSS is still The estimation of SSS fields is challenging in high latitude regions, and the quality precision of Soil Moisture and Ocean Salinity (SMOS) SSS retrieval was is improved by applying a threshold on SSS weekly error. The validity of SST and DMI (Danish Meteorological Institute) SST and SMOS SSS products is demonstrated thoroughly studied using ARKTIKA-2018 expedition continuous thermosalinograph measurements and CTD casts. The surface gradients and mixing of river and sea waters in the free of ice water in the ice-free and ice covered areas is are described with a special attention to the marginal ice zone at a synoptic scale. The Ekman transport was is calculated to better understand the pathway of surface water displacement. T-S We suggest that the freshwater is pushed northward, close to MIZ and under the sea ice, as it is confirmed by the oxygen isotopes analysis. The SST-SSS diagram using surface satellite estimates shows a showed the possibility to investigate the surface water masses transformation in detailat synoptic scales and reveal the presence of river water on the shelf of the East-Siberian Sea.

1 Introduction

The eastern part of the Eurasian Arctic remains one of the understudied less studied areas of the Arctic Ocean. The recent ARKTIKA-2018 expedition combined with novel satellite sea surface salinity and other parameters provide an unprecedented documentation of the temporal evolution of the surface water properties in the Laptev ? described this region as an "interior shelf" (Kara, Laptev, East-Siberian, together with Beaufort Seas), where 80% of the Arctic basin river discharge is released. The Arctic Ocean stores 11% of global river discharge, so its role in the planetary water budget merits attention with attention. Surface stratification and freshwater content are regarded as key parameters that have to be followed to better understand the changing state of a "New Arctic" climate (?). Overall, a freshening of the Arctic Ocean in 2000-2010 was reported in the American basin (?), and at the same time, a decrease in freshwater content of about 180km^3 between 2003 and 2014 was calculated from altimetry measurements by ?. ? discussed the salinification of the Laptev sea since 1989 up to 1997, explaining it by the eastward freshwater displacement and an excessive brine release in the sea ice leads. The importance of shelf seas for the freshwater content distribution was outlined in several recent studies (?, ?, ?), and its exchange with the deep basins is apparent (500 km^3 for the Laptev and the East-Siberian Seas ~~in summer 2018. The Laptev sea~~ with anticyclonic atmospheric vorticity, calculated from 1920-2005 hydrographic measurements "on quasi-decadal timescales" by ?).

The processes occurring at the Eastern Eurasian Arctic shelf are important, as the redistribution of this freshwater coming into this region and its further path is still unclear and its amount is supposed to increase (?). Complex topography, several sources of fresh and saline water masses, unstable atmospheric conditions and other parameters, like mesoscale activity and tidal currents, can alter the direction of this freshwater distribution. Close to the coast the riverine water from several sources is considered to propagate eastward as a "narrow (1-20 km) and shallow (10-20 m) feature" (?), but its transformation and mixing with saline sea water and sea ice melting and freezing is less studied. The Laptev Sea and the East-Siberian shelf areas were described as a substantial region of sea ice production for the central Arctic (?), and to better understand the impact of the incoming freshwater on the sea ice formation, the freshwater pathways in the Arctic should be understood better. Despite several studies on the freshwater in the Eastern Arctic (e.g., ?, ?, ?, ?), to the best of our knowledge, no study has shown yet the evolution of the water masses on a synoptic scale in the Laptev Sea.

The Laptev Sea is shallow in its southern and central ~~part (50-100~~ parts (less than 100 m) with a very deep opening ~~on~~ in the north (3000 m) ~~.~~ (Fig. 1). Several water masses are ~~mixing there~~mixed in the Laptev Sea. The Lena~~and the Khatangarivers~~ , the Khatanga, the Anabar, the Olenyok, and the Yana Rivers discharge fresh water in the shallowest part of the Laptev ~~sea on the south, the Kara sea~~ Sea in the south. The Kara Sea water enters via the Vilkitskiy and Shokalskiy straits, the Atlantic ~~water~~ Water (AW) ~~arrives~~ propagates along the continental slope to the north of the Severnaya Zemlya ~~archipelago~~ Archipelago and further eastward, the Arctic ~~water~~ Water exists in the northern part (?, ?, ?). The direction of surface freshwater circulation is supposed to correspond to the general displacement of the intermediate Atlantic Water (?). This eastward transport brings the water masses of the Laptev Sea over the shelf of the East-Siberian Sea where it comes under the additional influence of Pacific-derived waters (?, ?).

In the Arctic region, a strong ~~seasonal warming and cooling,~~ seasonality of air-sea heat fluxes with sea ice melting and freezing modify temperature and salinity in the upper layer, and therefore, ~~complexify the~~ result in a complicated vertical structure of water column ~~creating fronts at sea~~ with fronts at the surface and "modified layers" in the interior (?, ?, ?). ~~? and ? have shown that interannual changes of river discharge and wind patterns define the position of the oceanographic fronts in the central part of the Laptev Sea. To the best of our knowledge, no study has shown yet the evolution of the water masses on a synoptic scale in this region. In this study, we propose to follow the upper ocean waters displacement and its causes on a daily basis.~~

The most common concept of the upper ocean layer is a "mixed layer~~depth~~" ~~(MLD)~~ concept: between the ocean surface being in contact with the atmosphere and a certain depth, temperature and salinity are homogeneous. It ~~is defined via a certain~~ extends until a specified vertical gradient in density and/or temperature (?, ?), or the maximum of Brunt-Väisälä frequency

(?), or via the energy vertical distribution (?). For . In the Arctic, the reported mixed layer depth varies between 5-7 m and 30-50 (MLD) vary between 5 and 50 m depending on a region: region, time, and open water or under the ice , the Barents Seameasurements (10 m in the Laptev and East-Siberian Seas and 5 m in the Central Arctic ocean and Northern Barents Sea in summer, ?; 10-15 m in the Beaufort Sea close to MIZ in summer, ?; 20 m in the Barents Sea in late summer, ?, the East-Siberian Sea or the central Arctic (?, ?, ?, ?). 40-50 m under the ice close to the North Pole in winter, ?).

At the same time, the study of ? proposes to use for the Arctic ocean a ? proposed to use the term "surface layer" instead of the "mixed layer" for the Arctic Ocean, because the water horizon laying layer lying between the sea surface and the Arctic main halocline can be weakly stratified even though the halocline hampers an active exchange of matter and energy. The main halocline is situated at 50-100 m depth in the Eastern Arctic , ?, (?), and at 100-200 m depth in the Western Arctic ocean Ocean (?). Using the concept of "surface layer" with some assumptions, the processes above the mentioned depths in that layer can be discussed separately from the interior. ones in the deeper layer. The freshwater is supposed to be delivered to the central (European) Arctic from the Siberian shelf, roughly along the Lomonosov Ridge and to the western Arctic, partly along the continental slope.

The position of the pycnocline in the Arctic is mostly defined by the salinity. One of the first studies of ? devoted to the freshwater content was using 34.80 PSS as a reference salinity value separating the "fresh" and the "saline" waters, as at that moment it was a mean Arctic salinitywater; 34.80 was considered the mean Arctic Ocean salinity at that time. This value is used as well in more recent overviews (?). In the study of ? e.g. ?, ?), and helps to define the "Atlantic Water" as saltier than this value. ? used a depth of 34 PSS isohaline was used isohaline to estimate the liquid freshwater content in the Arctic ocean. ? based on in situ data in the Laptev sea for 1950-1993 and 2007-2012 periods reported Ocean. ? considered the depth of "near-freezing freshwater mixed layer" in the Eurasian Arctic Ocean to be 5-10 m. ? reported an overall salinity in the surface upper 5-50 m layer to lay within a within the range from 30.8 to 33 PSSbased on in situ data in the Laptev Sea during 1950-1993 and 2007-2012. Between the very surface layer and the Atlantic waters, ? finds out a modified Water, ? found a Modified "lower haloclineLower Halocline" waters Water with typical characteristics of salinity (between 33 and 34.2PSS) and negative temperatures temperature (below -1.5°C); in 2002-2009 this layer was situated at 50-110 m depths. A general depth. The study of ? on the Arctic ocean freshening defines Ocean freshening defined the upper ocean layer to be between 0 m and a depth of a density layer $\sigma_\theta = 27.35$ $kg \cdot m^{-3}$. This isopycnal is often located at 140–150 m depth, "slightly above the Atlantic water Water upper boundary defined by the 0°C isotherm". To analyse the upper-ocean processes, we will focus on the very surface with satellite data and on the upper 250 m layer with the CTD casts, showing the isohaline and isopycnal positions. Such approach to the

Mixing can be induced by winds generating surface-intensified Ekman currents, mesoscale dynamics (eddies), shear in tidal and other currents (?, ?, ?). The tidal currents and internal waves amplified over the shelf edge are associated with the mixing in the interior of the water column, below or in the main Arctic pycnocline (?, ?, ?). ? and ? showed that interannual changes of river discharge and wind patterns define the position of the oceanographic fronts in the central part of the Laptev Sea. Based on the model results, ? showed that in 1989-1997 the freshwater was driven eastward under the influence of winds associated with a "upper layerstrong cyclonic vorticity over the Arctic"is necessary to know the upper limit of the Atlantic waters, though not

~~being the subject of this study, but essential for the water mass transformation~~. The same study demonstrated that the associated salinification of the central Arctic Ocean weakens the vertical stratification of the water column. **?** discuss the importance of sea ice, as it creates a surface drag and establish the Ekman transport of the freshwater in the surface layer, which, in turn, impacts the dynamical ocean topography and geostrophic currents in the Arctic Ocean. **?** further mentioned that alongshore winds correlated with AO (Arctic Oscillation) index create the onshore Ekman transport, changing the water properties over the shelf.

Concerning the seasonal dynamics, the summertime is of a particular interest for all Arctic studies. The sea ice melting usually starts in June and ends in August-September, while the sea ice formation can start already in September and by November the Laptev Sea is covered completely. The East-Siberian Sea is covered by sea ice most of the year, and is exposed to the air-sea interaction for a shorter period of time (in August-September) over a smaller ice-free surface than the Laptev Sea. August and September are two summer months that are very important for the heat exchange between ~~the~~ open ocean and atmosphere over the Laptev ~~sea~~Sea. In a recent study, **?** reported that during this time period when the sea ice is melting and the ocean is opening, ~~a radiative balance~~ the net radiative balance at the sea surface changes from 100 W/m^2 to ~~negative~~ zero values, following the seasonal cycle of shortwave radiation (meaning the flux from the atmosphere to the ocean). The sea level anomalies over the Eastern Arctic shallow seas are positive and largest in summer (up to 10 cm at 75°N, down to 3 cm at 80°N, as it was reported by **?**). ~~The Laptev sea considered in this article~~

The Laptev Sea is not at all sampled by Argo products, so the recent ARKTIKA-2018 ~~measurements offer a good opportunity to validate SST and SSS. Accurate measurements of surface salinity can enrich our understanding of freshwater content in the Arctic (**?**) and SSS estimates from L-band satellites can bring a valuable input.~~

~~In this paper,~~ expedition measurements combined with novel satellite sea surface salinity and other satellite-derived parameters provide an unprecedented documentation of the temporal evolution of the surface water ~~evolution of~~ properties in the Laptev and ~~the~~ East-Siberian ~~seas will be described and analysed considering wind speed and direction during the period of the ARKTIKA-2018 expedition. Firstly, data and methods used for the following study will be presented. Then, we compare SST and SSS satellite estimates with in situ measurements. The influence of the wind speed on Laptev sea is discussed considering Ekman transport and pumping. Finally,~~ Seas during the summer 2018. In this study, we propose to follow the upper ocean water displacement and to discuss what causes it on a daily basis.

2 Data and Methods

To analyse the upper-ocean processes, we will focus on the very surface with satellite data and on the upper 250 m layer with the CTD (conductivity, temperature, depth) casts, showing the isohaline and isopycnal positions. Such an approach to the upper layer is required to estimate the upper of limit of the Atlantic Water, which is one of the key contributors to the ~~better understanding allows to describe the water masses~~ water mass transformation. The surface water evolution of the Laptev ~~sea and their transformation during August-September 2018.~~ and the East-Siberian Seas is described and analysed considering wind speed and direction during the ARKTIKA-2018 expedition.

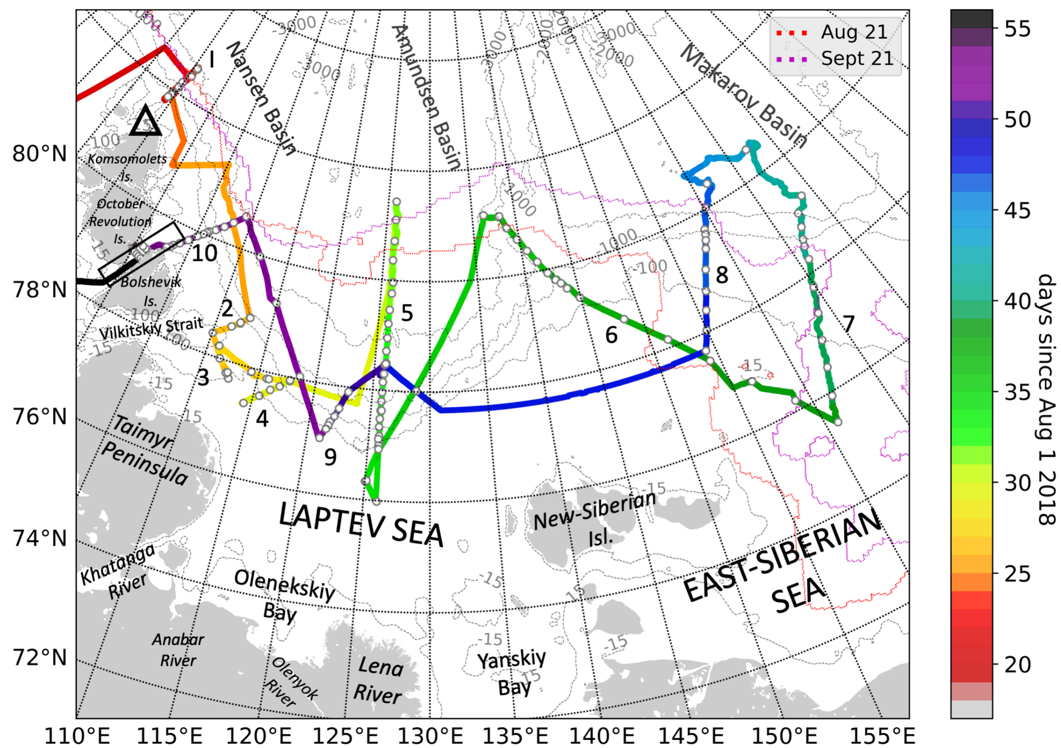

Figure 1. Legs and stations of the ARKTIKA-2018 expedition overlayed on the bathymetry from ETOPO1 "1 Arc-Minute Global Relief Model" (?). CTD stations are shown with white dots. The color indicates the number of days since August 1, 2018. The sea ice edge position is indicated with a red dashed line for the beginning (August 21) and with the purple dashed line for the end of the expedition (September 21). The ice edge is based on the sea ice mask provided in the SST DMI product. Numbers indicate positions of 10 oceanographic transects discussed below. The black triangle in the north of the Komsomolets Island shows the Arkticheskiy Cape. The Severnaya Zemlya Archipelago consists mainly of the Komsomolets, the October Revolution, and the Bolshevik Islands (with smaller islands not shown here). The black box indicates the Shokalskiy Strait between the October Revolution and the Bolshevik Islands. The Yana river estuary is situated southward the Yanskiy Bay (out of the map).

3 Data and Methods

2.1 In situ measurements during the ARKTIKA-2018 expedition

Oceanographic measurements during the ARKTIKA-2018 cruise expedition on board RV Akademik Tryoshnikov started on August 21, 2018 and ended on September 24, 2018 (Fig.1). Standard oceanographic stations (145 in total) were conducted with Sea-Bird SBE 911plus CTD instrument. Oceanographic sections were organized in the way to best represent the processes between the to take into account the interests of different scientific expeditions on board, NABOS (Nansen and Amundsen Basin Observational System) and CATS (Changing Arctic Transpolar System) to observe shallow and continental slope areas, but also processes. NABOS sections were mostly cross-shelf (1, 5, 6-8, 10), and CATS sections were shallower (2-4, 9). Section 3 and 10 were made in the straits between the Kara and the Laptev sea: Sea: the section 3 in the Vilkitskiy Strait southward to the Bolshevik Island, with depths from 70 to 1500 and the 200 m opening into the deep central part of the Laptev Sea (more than 1000 m) and the section 10 in the narrow and rather shallow (250 m) Shokalskiy Strait between the Bolshevik and the October Revolution Islands. Part of the Some measurements were carried out in marginal ice zone (MIZ) and ice-covered area . (see the sea ice edge positions at the beginning and the end of the cruise in Fig.1). In this study we define MIZ as an area with 0-30% sea ice concentration close to the ice edge. Standard oceanographic stations (145 in total) were conducted with SeaBird SBE911plus CTD instrument equipped with additional sensors. For this study, we use mainly the CTD measurements of potential temperature and practical salinity, but also the results of oxygen isotope analysis from the first (surface) bottle samples (?). All CTD data were processed and quality checked. The cruise data can be found at https://arcticdata.io/catalog/data (?) and ?.

The ship was equipped with an underway measurement system Aqualine Ferrybox, widely known as a thermosalinograph, TSG. The instrument had a temperature and a conductivity (MiniPack CTG, CTD-F) sensors and a CTG UniLux fluorometer installed; thus, continuous temperature, salinity and chlorophyll-a estimations were obtained along the ship's trajectory. The inflow is situated at 6.5 m below the surface (the inflow hole is on the ship's hull). All data were processed and filtered for random noise and bad quality datameasurements, and then compared and calibrated with CTD measurements. Standard ongoing meteorological measurements of wind speed and direction make it possible to partly assess the impact of real atmospheric forcing. When calculating a linear regression between CTD measurements at 6.5 meters depth and TSG measurements, we obtain a good correlation for both temperature and salinity (correlation coefficient equal to 0.979 and 0.966, respectively, not shown). The standard error is 0.023 for temperature and 0.025 for salinity, and the standard deviation for the difference of measurements (CTD minus TSG) was $STD_{temp} = 0.413$, and $STD_{sal} = 0.423$. To adjust the continuous TSG measurements to the more precise CTD measurements, we applied the obtained linear regression equation to TSG data. We only use these adjusted temperature and salinity data.

The vertical profiles of the conservative temperature and practical salinity in the upper layer are presented in Fig.2. To investigate if the TSG measurements can be used to study the surface layer in a highly stratified Laptev sea, we calculated a summer mixed layer depth following **?** method based on density and temperature gradient thresholds (Fig.2, a, c). The MLD is found at a depth of the first maximum temperature gradient below a depth of defined (by given threshold) density gradient (see **?** for details). Using the same approach, we computed MLD with density and salinity vertical profiles. The threshold chosen for practical density gradient was 0.3 kg/m^3 per 1 Arc-Minute Global Relief Model" (?). CTD stations are shown with white squares. Color bar indicates the number of days since August m, and 0.2 salinity units per 1 , meter for conservative temperature and practical salinity gradients. Regarding the MLD calculated from salinity (MLD_{sal}), most of the measured vertical profiles (75.17%) had the MLD_{sal} below 7 m depth with the median of MLD_{sal} 11.99 m. As for the temperature (MLD_{temp}), 81.37% of the measured profiles had the MLD below 7 m depth with a median of $MLD_{temp} = 13.50m$. Thus, in most cases the upper 12 m of the surface layer was homogeneous, and our CTD and TSG measurements can be used for the validation of satellite data. The median vertical profiles of temperature and salinity in the upper 5-100 m are presented as

~~Time of the ARKTIKA-2018 expedition works and bathymetry from ETOPO1~~

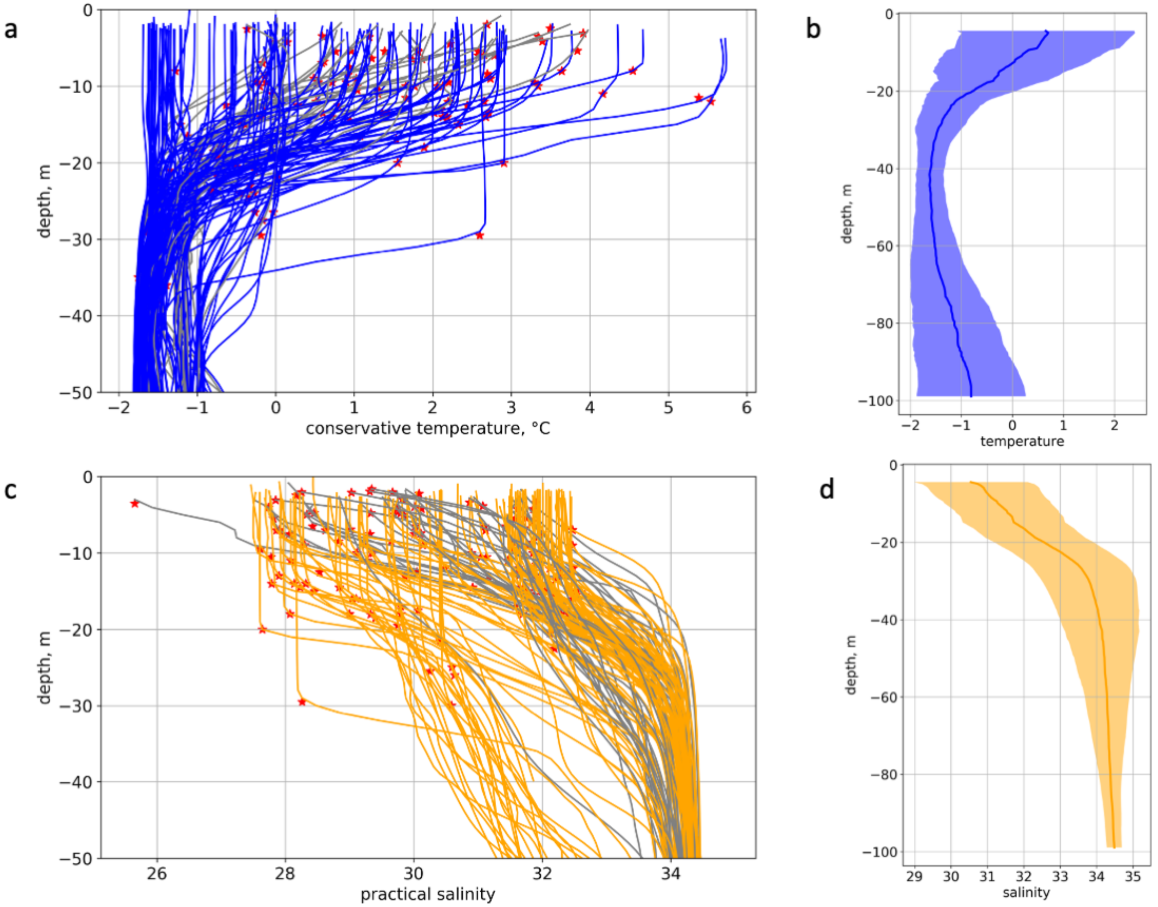

Figure 2. Vertical profiles of conservative temperature (a, b) and practical salinity (c, d) from CTD measurements in the upper ocean layer. Figures (a) and (c) show all vertical profiles in the upper 50 m, where red stars indicate the mixed layer depth, calculated using **?** method (see details in the text), colored profiles show the cases, when the MLD is below 7 m depth and gray profiles indicate when the MLD is above 7 m depth. Figures (b) and (c) show the median vertical profiles of temperature and salinity in the 5-100 m layer, respectively, where the shaded area shows the associated STD.

well as the associated STD in Fig.2, b, d). We observe rather cold (0.5°C) and fresh (30.5) water at 5 m, followed by a smooth thermo- and halocline down to 30 m depth (with a temperature of -1.3°C and salinity of 33.8). Below 30 m the temperature is slightly rising to -1 °C, and salinity stays close to 34.5. The STD of conservative temperature is the largest at the surface (1.55°C) and smallest at 40 m depth (0.27°C). The STD of salinity is also the largest at the surface, 1.50, but is diminishing with depth to 0.20 at 100 m. Nevertheless, it is clear that at the end of a summer season in the region with very different water origins, these median profiles are not representative for all water masses. Additionally, we did an important number of CTD casts in very shallow areas with depths between 30 and 50 m, so the calculated averaged (median) vertical profile is a composite

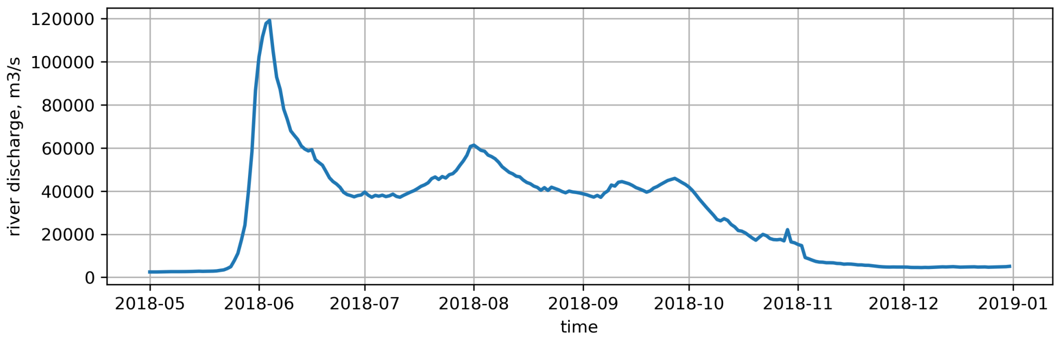

Figure 3. The ~~sea ice edge positions are indicated with a dashed lines for the beginning (August 21) and the end of expedition (September 21). The numbers indicate 10 transects that will be studied later~~ Lena River discharge in ~~the paper.~~2018, data from Arctic GRO dataset (https://www.arcticrivers.org/data)

of "shallow" and "deep" vertical profiles. We do not include the very surface measurements above 5 m, because we had only 45 CTD measurements at 2 m depth among 146 possible, and taking them into account would bias the median profiles as well.

2.1.1 River discharge

To illustrate the amount and temporal variability of the river discharge in 2018, we used daily measurements of the Lena River discharge from the Arctic Great Rivers Observatory (GRO) dataset (https://www.arcticrivers.org/data)). In Fig.3 we present a time series of the Lena River discharge from May to November 2018. The river stayed under the ice with a very small discharge up to the end of May. The main peak of the Lena River discharge occurred in the beginning of the Arctic summer in June and corresponds to the snow and ice melting over the river basin in Siberia. In two weeks, the discharge changed from 2 500 to 120 000 m^3/s. The second, smaller peak of the river discharge occurred in the beginning of August (60 000m^3/s), which might be associated with the summer precipitation. In August 2018 the river discharge was decreasing from 60 000 to 40 000 m^3/s, and in September it varied very little staying close to 40 000 m^3/s. A significant diminution of the river discharge started in the beginning of October and continued up to the beginning of November. After the beginning of November the river discharge was very weak and close to its minimum values (4500 m^3/s).

The described seasonal dynamics is typical for the Lena River and consistent with existing results, e.g. demonstrated in **?**. It can be complemented by the results of **?** study of the large Siberian rivers using satellite data. **?** showed that the maximum of precipitation over the basins of the Lena, the Ob' and the Yenisey Rivers occurs in July, and the mean monthly air temperature is maximum at this time.

2.2 Satellite data

Satellite data provide an instant information about surface distribution of geophysical characteristics over the whole study area and together with their temporal evolution.

All listed below products were products listed below are considered from August 1, 2018 to September 25, 2018 (the last day of ARKTIKA-2018 expedition). If not indicated additionally, for consistency all products were For consistency, when not specifically indicated all products are linearly interpolated on a regular grid within the bounding box 74-85N 90-170E, with 0.01 degree step in latitude, and 0.05 degree in longitude. The spatial resolution of selected grid roughly corresponds to 1 kmon the studied latitudes.

2.2.1 Sea surface temperature

2.2.2 Sea surface temperature

The SST-retrieving instruments with the highest resolution, such as AVHRR , MODIS and VIIRS (Advanced Very High Resolution Radiometer), MODIS (Moderate Resolution Imaging Spectroradiometer) and VIIRS (Visible Infrared Imaging Radiometer Suite) work in Near Infrared (NIR) and Infrared (IR) bands and depend strongly strongly depend on atmospheric conditions (provide providing measurements for clear sky). For lower resolution microwave instruments, such as AMSR2 (Advanced Microwave Scanning Radiometer 2), the clouds are not opaque, but SST retrieval transparent, but the SST retrievals may still be hampered by high wind speed and precipitation events. As satellite measurements in IR and NIR ranges are sparse because of the frequent cloudiness over the Arctic ocean, a use of a blended productcan be favorableOcean, we used a blended product. In this paper we use the Danish Meteorological Institute Arctic Sea and Ice Surface Temperature product (hereafter referred as "SST DMI"). SST DMI is a Level 4 daily product provided by the Copernicus Marine service ("Level 4 product" means that several swath measurements were interpolated to achieve a regular resolution in time and space). Daily surface temperatures over the sea and ice are calculated derived on a 5 km spatial grid from several instruments: AVHRRand , VIIRS for SST and AMSR2 for sea ice concentration, using optimal interpolation (**?**).

Besides the full coverage over the studied area, the advantage of the blended SST DMI product is that it takes into account the ice temperature, so the marginal ice zone (MIZ) is better represented and not masked out. The total number of SST measurements ingested over the studied area from August 1 to September 25, 2018 varies from 1000 to 2500 measurements per pixel.

2.2.3 Validation of SST DMI

The first step of the SST DMI validation was its value-by-value comparison with a collocated in situ dataset (nearest neighbour SST DMI pixel). For this analysis, we co-embarkinglocated SST DMI with the in situ potential temperature measurements in the upper 6.5 m layer: all available CTD measurements averaged every half a metre above 6.5 m depth and all TSG measurements at 6.5 m depth averaged every 30 minutes. The median depth of the collocated CTD measurements is 5.25

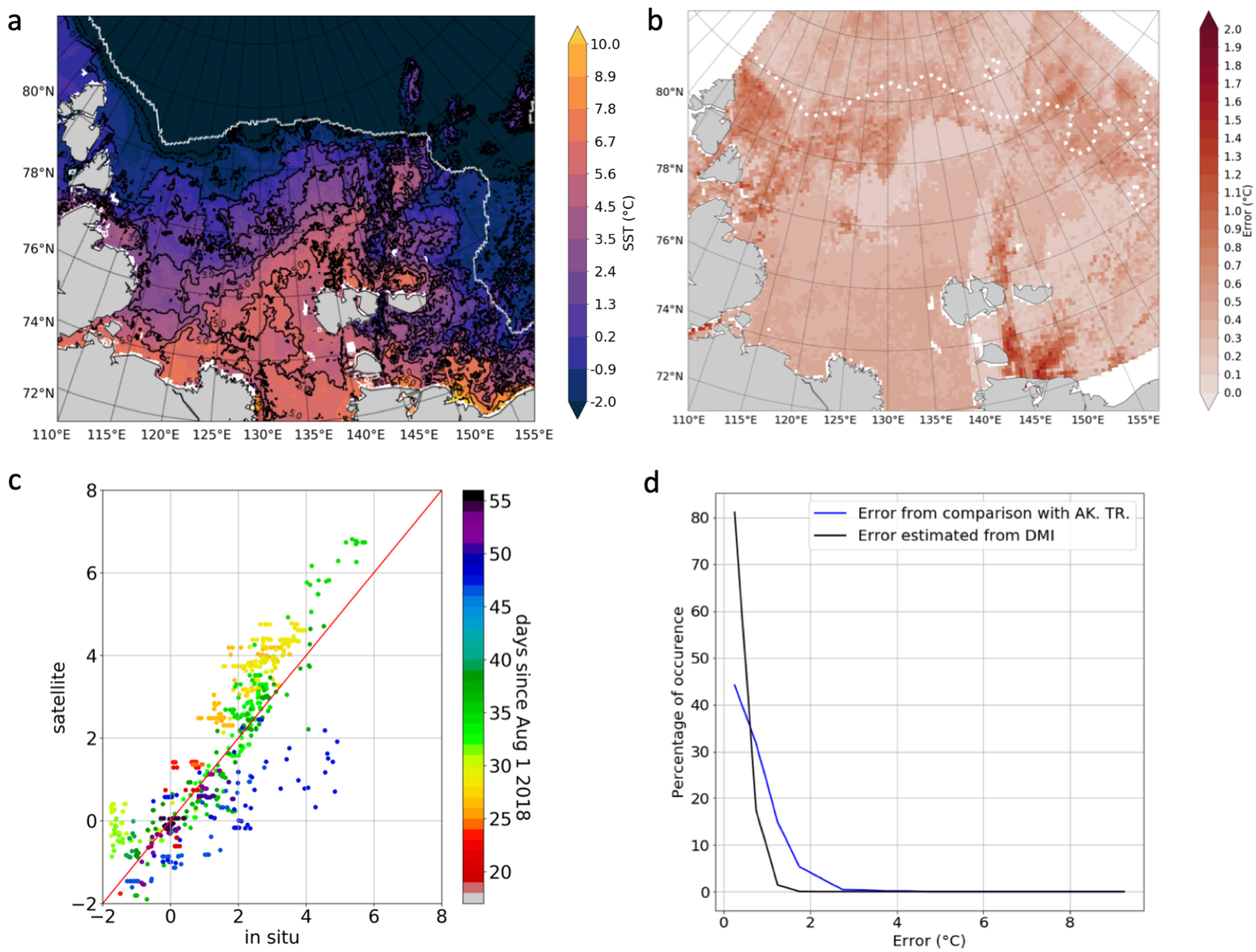

Figure 4. Sea surface temperature validation: example of SST DMI L4 image for September 13 (a) with the error estimates (b); comparison of collocated SST and in situ data (CTD and TSG) in the upper 6.5 m (c) and distribution of error provided by DMI and absolute difference derived from comparison with in situ data (d).

m. As for the TSG, the ship was moving with a median speed of 8 knots during the cruise, so an average of 30-minutes TSG measurements is an average over approximately 7.5 km. Thus, 30-minutes TSG average is comparable with one SST DMI pixel (10 km). There were 1707 collocated points in the analysis.

Although, in fact, satellite SST estimates may differ from the in situ temperature measurements in the upper 6.5 m, we expect some overall consistency between the datasets. Studies carried out by **?** devoted to the validation of MODIS SST in the MIZ, and by **?**, which described in situ measurements in the iced-covered area, reported that the first 7-10 m layer below the surface was mostly homogeneous. As it is shown in Fig.2, most of our measurements (more than 75%) were homogeneous in the upper

12 m (and were done in the ice-free areas). Nevertheless, a diurnal warming and a local vertical mixing can affect the vertical temperature distribution in the very surface layer. The SST diurnal amplitude can reach more than 3 K in the Arctic Ocean (**?**). To create SST DMI L4 product, only the observations between 21:00 and 7:00 local time are used (**?**), thus, local diurnal variations of SST are supposed to be filtered out. Diurnal variation of temperature might be present in real in situ measurements in case of strong diurnal warming events, but no particular observations allowing to investigate this question were done during the cruise.

To illustrate the consistency of SST and in situ temperature datasets, September 13, 2018 was considered as it was one of the rare days in summer 2018, when the central part of the Laptev Sea was cloud-free, which is especially important for SST DMI.

The SST DMI product for September 13, presented in Fig. 4 (a) shows a rather complex pattern with a pronounced gradient associated with warm river water in the central part of the Laptev Sea. The error in SST estimates provided by DMI, is shown in Fig.4 (b, d). The percentage of occurrence is computed in temperatures classes with a size of 0.5 degrees that starts at 0 degrees (Fig.4, d). The highest potential error (up to 2.5°C), was observed over some open sea areas (due to potential cloudiness), but was mostly associated with the sea ice due to its heterogeneity (Fig.4 (b)). Over most of the southern and the central part of the ice-free Laptev and the East-Siberian Seas, the error is below 0.5°C and over the eastern part, it is below 1°C.

Comparison of the SST DMI and in situ surface-layer temperature (Fig. 4, c) shows a very good agreement almost independent on area and time during the ARKTIKA-2018 expedition. The correlation coefficient is 0.89, and the RMS is 0.77°C. The difference between mean in situ and mean SST DMI data is -0.19°C, where the SST DMI is higher than the in situ temperature. This value seems to be realistic, as the CTD data justifies it. According to CTD measurements, the 0-3 m water layer is on average 0.3°C warmer than the 3-6.5 m layer (not shown). The largest deviations are observed when the expedition is working in the MIZ or more compact sea ice, so they might be associated with either imperfect sea ice flagging of some stages of sea ice in the SST DMI product or a noise introduced after re-interpolation of data on a regular grid. This noise together with the different sampling of in situ potential temperature measurements and SST DMI product lead to a standard deviation of the difference between in situ and SST DMI larger than the error provided in the SST DMI product (Fig. 4, lower right). Overall, SST DMI agrees well with in situ data, so we use this product for the following analysis of SST time-series.

2.2.4 Sea surface salinity

Soil Moisture and Ocean Salinity (SMOS) ~~was~~ is the first satellite mission ~~embarking~~ carrying an L-band (1.41 GHz) interferometric microwave radiometer, which measurements ~~make possible to derive~~ are used to retrieve the sea surface salinity (SSS). With recent processing, the standard deviation of the differences between 18-day SMOS SSS and 100-km averaged ~~ship SSS~~ TSG surface salinity measurements is 0.20 ~~PSS~~ in the open ocean between 45°N and 45°S (~~?~~**?**). However, the precision degrades in cold water as the sensitivity of L-band radiometer signal to SSS decreases when SST decreases, even though this effect on temporally averaged maps is partly compensated by the increased number of satellite measurements at high latitude. A possibility of using SSS estimates in cold regions derived from L-Band radiometry ~~was, however,~~ has been demonstrated recently by several working groups (**?**, **?**, **?**). However, existing L3 ("Level 3" means a product resampled at a uniform time-spatial grid, different from swath grid) SSS products: SMAP CAP/JPL (Soil Moisture Active Passive satellite, a product created using the Combined Active Passive algorithm by Jet Propulsion Laboratory) SSS or SMOS BEC ~~L3 products~~ (Barcelona Expert Center) SSS, are spatially averaged from 60 km to more than 100 km.

~~Soil Moisture Active and Passive (SMAP) L3 SSS~~ SMAP REMSS (Remote Sensing Systems) SSS L3 v3 ~~from REMSS provides a 40km resolution version~~provides a 40 km resolution version, but do not provide a sufficient coverage in the Laptev Sea. The methodology developed in this study ~~for retrieve SMOS weekly~~ to retrieve SMOS SSS aims at maintaining SMOS ~~SSS~~ original spatial resolution and at ~~attempting to retrieve~~ retrieving SSS as close as possible ~~from~~ to the ice edge.

~~Weekly SSS average~~ A new product, hereafter SMOS SSS "A" ("A" for the Arctic Ocean) L3, investigated in this study ~~are~~ was computed using SMOS ~~SSS~~ L2 ("Level 2" product means that a geophysical parameter, eg. SSS, was computed at the swath grid) SSS from the ESA (European Space Agency) last processing (v662, **?**). SMOS L2 SSS are available on the ESA SMOS Online Dissemination website. The mean spatial ~~resolution of individual SMOS SSS~~ (radiometric) resolution of SMOS product is close to 50 km~~. SMOS~~ , but SMOS ESA L2 SSS products are ~~sampled~~ oversampled over an Icosahedral Snyder Equal Area (ISEA) grid at 15 km resolution. ~~Seven days running means are computed each day in each pixel . SSS are temporally weighted using a Gaussian~~

SMOS "A" SSS was obtained as described below. Seven-day running means were computed for each day and each pixel of the ISEA grid, with a temporal Gaussian weighting function with a standard deviation of 3 days. The full width of SMOS ascending and descending orbits swaths ~~is~~ was considered in order to take advantage of better temporal and spatial sampling over the Arctic ~~ocean and~~ Ocean and to decrease the uncertainty with temporal averaging. In order to eliminate the SSS at very low and high wind speeds because of ~~their~~ its high uncertainties, SMOS ~~SSS are~~ ESA L2 SSS was considered only if the associated ECMWF ~~wind speeds are~~ (European Centre for Medium-Range Weather Forecasts) wind speed was between 3 and 12 m/s. ~~SSS measurements are also weighted by~~ SMOS ESA L2 SSS measurements were also weighted relative to the estimated error of the SSS measurement (as in (**?**, equation A7). This error ~~is~~ was derived from the SSS theoretical error multiplied by the normalized χ^2 cost function. **?** ~~have shown that the Klein and Swift (**?**)~~ showed that the **?** dielectric constant model ~~is~~ was inaccurate at low SST. In order to mitigate this effect, a SST-dependent correction derived from the Fig. 16 of **?** (blue-circle line) ~~has been applied.~~ was applied: $SSS_{SMOS-"A"} = SSS_{SMOS-ESA-L2} - (-5\cdot 10^{-4}\cdot SST^3_{ECMWF} + 0.02\cdot SST^2_{ECMWF} - 0.23\cdot SST_{ECMWF} + 0.69)$. Finally, a ~~criteria on~~ criterion on a SMOS-retrieved pseudo-dielectric constant (ACARD parameter~~) is~~ , defined in **?**)) was applied to discard SMOS measurements affected by sea ice (discarded when $ACARD < 45$). The error ~~on the weekly SSS mean is~~ of SMOS SSS "A" was derived from the propagation of the error on individual ~~SSS. It~~ SMOS ESA L2 SSS pixel during 7 days. The error increases strongly in the vicinity of sea ice. For this reason, in the following study, above 75°N, all pixels with ~~a~~ an SSS weekly error larger that 0.8 ~~PSS are~~ were not considered. South of 75°N, a higher threshold ~~is~~ was used (1.5~~PSS~~) allowing to maintain some measurements ~~close from the source of the river plume where the~~ closer to fresh river water from the Lena and the Khatanga Rivers near the coast. In this area, the χ^2 may increase due to the strong heterogeneity of SSS within SMOS multi-angular brightness temperatures footprints~~and where~~ , and the number of measurements is low due to the ~~combined~~ presence of the coast and islands ~~but without ice sheet.~~ even without sea ice. A theoretical error of SMOS SSS "A" field is below 0.5 in the center of the Laptev Sea and up to 2 and higher close to the coastline and MIZ.

2.2.5 Validation of SMOS "A" SSS

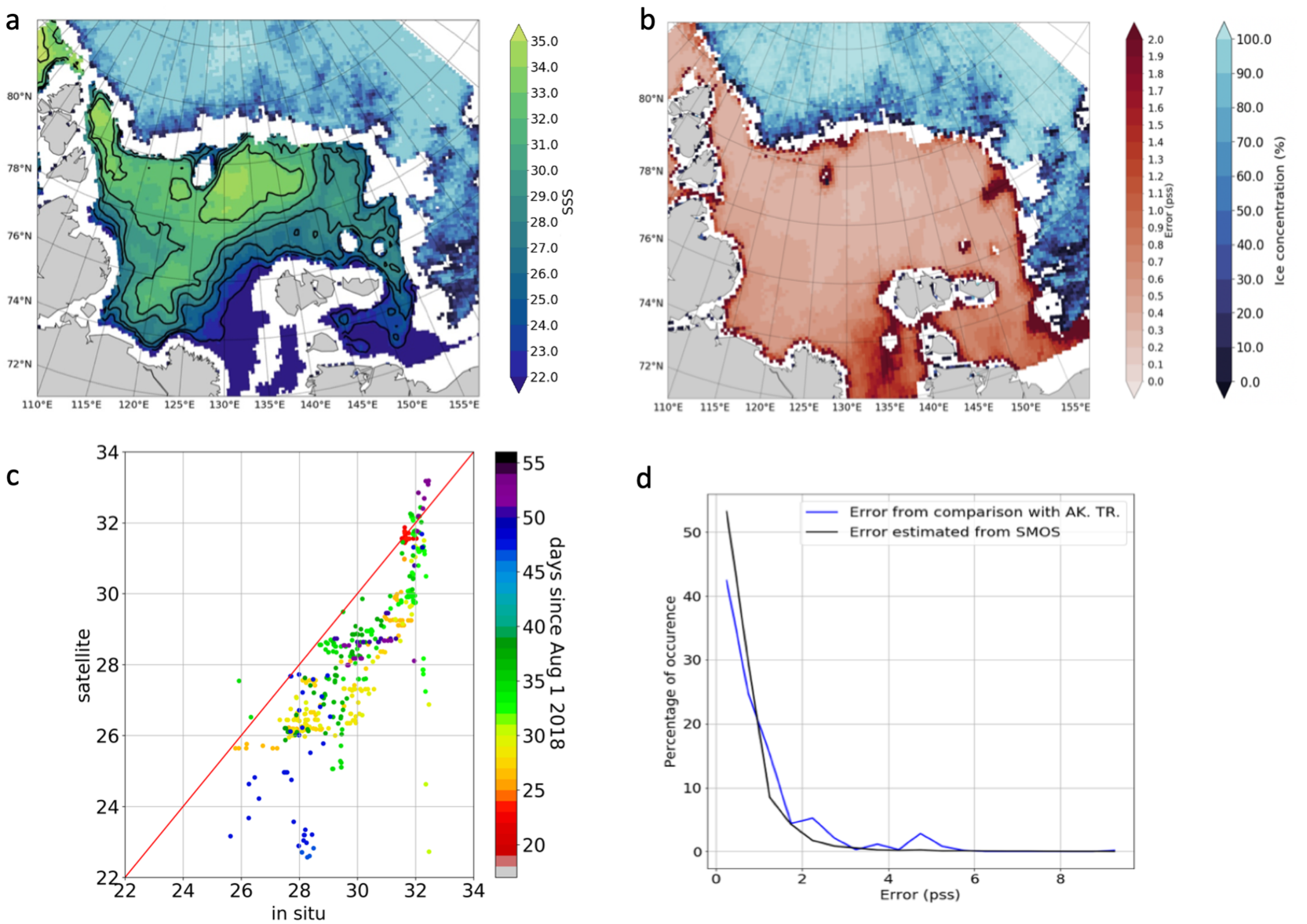

Figure 5. Sea surface salinity validation: example of SMOS SSS "A" for September 13, 2018 (a), computed error estimates for this day (b), comparison of co-located SSS and in situ data in the upper 6.5 m (c) and distribution of provided SMOS L2 error and measured absolute difference from comparison with in situ data (d). Sea ice concentration from AMSR2 is indicated with blue shading on the upper panels

In this section, we compared the SMOS SSS "A" relative to in situ measurements. Figure 5 presents the SMOS SSS "A" on September 13, 2018, the same day as the DMI SST in Fig.4. We carried a co-location of SMOS SSS "A" and in situ measurements of salinity in the upper 6.5 m layer in a following manner: the averaging of the TSG salinity was done over one hour period (equal to ∼ 15 km distance, contrary to DMI SST validation) in order to be closer to SMOS SSS "A" spatial resolution. We used 985 collocated points.

Comparison between the in situ practical salinity and SMOS SSS "A" shows a very good agreement, not yet demonstrated before by any other salinity product in the Laptev Sea. The correlation coefficient is 0.86 with a RMS = 0.86. The mean difference is 2.06. In what follows, we subtract this mean difference from the entire SMOS SSS dataset. The standard deviation of SMOS SSS with respect to in situ SSS does not vary with the depth of the in situ salinity measurements above 6.5 m, either because in situ salinity was homogeneous vertically or because comparisons were too noisy to detect this small variations (not shown). Although SMOS SSS "A" shows a good agreement most of the time, some larger errors occur close to the ice margin or when pixels are contaminated by small ice pattern not detected by AMSR2 sea ice concentration algorithm (as at 80°N 125°E in Fig. 5, a).

Comparison between SMOS retrieved error and error based on comparison with in situ salinity measurements is presented in Fig. 5 (d). The percentage of occurrence is computed in salinity classes with a size of 0.5 that starts at 0. It shows a good agreement between the distribution of SMOS SSS "A" error estimated from retrieval process and the distribution of error obtained from comparison with in situ salinity measurements. This results allow us to use the SMOS SSS "A" error with confidence in our further analysis. Using error filtering, the points too close to the ice edge were excluded.

2.2.6 Sea ice concentration and ice masks

Sea ice masks were obtained from AMSR2 sea ice concentrations products provided by the University of Bremen (**?**): they are weather-independent, thus, continuous for ~~all time~~ the whole period. The highest available spatial resolution is 3.125 km. The AMSR2 ice masks were used in addition to the masks provided with every satellite product discussed (DMI SST, SMOS SSS "A", ASCAT (Advanced SCATterometer) winds L3 (see its description below)). A continuous erroneous presence of ice along the Siberian coast was observed and had to be filtered: images in optical band and the ice charts from the Arctic and Antarctic Research Institute (AARI) were used as a reference. As ~~detailed in section 2.2.2, additional filterings were~~ it was detailed above, an additional filtering was applied to SMOS SSS ~~as~~ "A" as the L-Band measurements are sensitive to ice thicknesses less than 50 cm contrary to AMSR2 measurements.

The sea ice opening starts relatively late in the Laptev Sea: a coastal polynya appeared in the southern-central part of the Laptev Sea at the beginning of June in 2018 and by the beginning of August, the sea was ice-free only south of 79°N. The Laptev Sea was completely covered by the beginning of November in 2018. For this study, we define the sea ice edge with the position of 1% sea ice concentration and MIZ as 0-30%.

2.2.7 Wind speed

To investigate the ~~winds speed patterns, we used~~ wind speed pattern, we use ASCAT scatterometer daily C-2015 L3 data produced by Remote Sensing Systems. Data are available at www.remss.com. ~~"~~

2.3 Reanalysis data

Reanalysis data ~~were~~ are used to include some additional parameters not available from satellite and in situ data. Atmospheric forcing fields~~-~~: sea level pressure, SLP, and air temperature, ~~were~~ are obtained from the ERA5 reanalysis (**?**). The latest reanalysis of ERA5 ~~yet have~~ still has relatively crude spatial grid of 0.5°for the SLP and 0.25°for air temperature.

3 Results

2.1 Comparison of datasetsEkman transport

To illustrate the consistency of the different satellite products, September 13, 2018 was considered as it is one of the rare days in summer 2018 when the central part of the Laptev sea was cloud-free, which is especially important for SST. investigate the role of the wind forcing, we compute mean monthly wind fields and the Ekman transport for August and September 2018. Horizontal Ekman transport, m^2/s, is calculated as:

$$u_{Ekm} = \frac{\tau_v}{\rho_w * f} \quad v_{Ekm} = -\frac{\tau_u}{\rho_w * f} \tag{1}$$

where u_{ekm} and v_{ekm} are horizontal components of the Ekman transport, τ is a wind stress, calculated from ASCAT winds (u_{wind}, v_{wind}) using ERA5 air density ρ_{air}: $\tau_u = C_D * (u_{wind}) * u_{wind} * \rho_{air}$; ρ_w is a surface density, calculated from SST and SSS with TEOS-2010 (?); C_D is surface drag coefficient calculated from wind speed according to ?: for the wind speed U_w below 10 m/s $u_{star} = 0.051 * U_w - 0.14$ and for the stronger winds: $u_{star} = 0.051 * (U_w - 8) + 0.27$; f is the Coriolis parameter.

The Ekman pumping (upwelling and downwelling) was computed as:

$$w_{ekm} = \frac{1}{\rho_w * f}\left(\frac{d\tau_v}{dx} - \frac{d\tau_u}{dy}\right) + \frac{\beta * \tau_u}{\rho_w * f^2} \tag{2}$$

where w_{ekm} is the Ekman vertical velocity and β is the y-derivative of the Coriolis parameter.

2.1.1 Temperature

The SST field from DMI L4 product for September 13, presented in Figure 4 shows a rather complex pattern with a pronounced gradient associated with river waters in the central part of the Laptev sea. Besides the full coverage over the studied area, the advantage of blended DMI product is that it takes into account ice temperatures, so the Marginal Ice Zone (MIZ) is better represented and not masked out. The total number of SST measurements ingested by SST DMI L4 over the studied area from August 1 to September 25, 2018 varies from 1000 to 2500 measurements per 1 pixel over the whole studied period. The error in temperature estimates provided by DMI, is shown on Fig.4. The highest potential error (up to 2.5°C), though observed over some open sea areas (due to potential cloudiness), is mostly associated with the sea ice due to its heterogeneity. Over most of the southern and the central part of the free-of-ice Laptev and the East-Siberian seas, the error is below 0.5°C and over the eastern part, it is below 1°C for selected day.

3 Results

The first step of satellite and in situ dataset evaluation was a value-by-value comparison of collocated dataset (nearest neighbor) and calculation of basic statistics. For this analysis, we collocated satellite-estimated temperature with the in situ measurements in the upper 6.5 m layer: CTD averaged every half a meter above 6.5 m depth and TSG at 6.5 m depth averaged every 30 minutes. The median depth of the collocated temperature measurements is 5.25 m due to the absence of CTD data in the very first meters. As the ship was moving with an average (median)speed of 8 knots, 30 minutes averaged TSG's temperature corresponds to the median of measured temperature over approximately 7.5 km, which is comparable with the spatial resolution of DMI SST L4 10 km. There were 1707 points in the analysis.

3.1 Overview of SST and SSS in the Laptev and East-Siberian Seas in August-September 2018

Though, in fact, satellite sea surface temperature estimates may differ from the measurements at 6.5 m, we expect some general consistence between the datasets. Studies carried out by **?**, devoted to the validation of MODIS SST in the MIZ and that one by **?** which describes in situ measurements in iced-covered area, report that the first 7-10 m layer below the surface is mostly homogeneous. Nevertheless, diurnal warming and local vertical mixing can affect the temperature distribution of in the very surface layer. Local diurnal variations of temperature are supposed to be filtered out in the blended DMI product, as it only uses observations between 21: 00 and 7:00 local time (**?**), but can still be present in real in-situ measurements.

Comparison of the DMI SST and in situ surface-layer temperature (Fig. 4) shows a very good agreement almost independent on area and time during ARKTIKA-2018 expedition. The correlation coefficient is 0.89, and the RMS is 0.77C. The bias between mean in situ and mean DMI SST data is -0.19C, where the SST is higher than the in situ temperature. This value seems to be realistic, because according to CTD and TSG measurements, in average, the 0-3 m water layer is by 0.3 degree warmer than the 3-6.5 m layer. The largest deviations are observed when the expedition was working in the MIZ or compact sea ice, so they might be associated with either imperfect sea ice flagging of some stages of sea ice in the blended DMI "SST and sea ice temperature" product, or an introduced noise after re-interpolation of data on a regular grid. This noise together with the different sampling of SST by in situ and DMI L4 product lead to a standard deviation of the difference between in situ and DMI SST larger than the error provided in the DMI product (Fig. 4, lower right). Overall, DMI L4 blended SST agrees well with in situ data, so we use this product for the following analysis of SST time-series.

4 Overview of SST and SSS in the Laptev and East-Siberian seas in summer 2018

The mean SST during the 2 summer months is 2.181 2.18°C in the Laptev sea (between Severnaya Zemlya archipelago and Sea (between the Severnaya Zemlya Archipelago and the New Siberian Islands), and 1.126 1.13 °C in the studied part of the East-Siberian sea Sea (Fig. 6). The highest temperatures (above 6°C, up to 9°C) were observed close to the Lena river River delta in the Yanskiy Bay and in the Olenekskiy Bay in front of the Khatanga river River. A warm water pool associated with the river plume between 125°E and 135 °E progressively propagates northeast and warms up this part of the sea: 0°C isotherm at 140°E meridian is situated 100 km northward compared to its position at 120°E. The studied part of the East-Siberian ~~sea~~ Sea was not completely ~~free of ice~~ ice-free in August-September 2018. Negative temperatures are observed near the ice edge at a distance of 50-100 km almost everywhere, except for a small area at 80°N 160°E, where warm river water meets the sea ice and no open water with negative temperatures is seen. The strongest gradients are observed along the sea ice edge and the river ~~waters~~ water plume (up to 0.05° C/km, gradient). Standard deviation ~~on~~ of SST in Fig.6 ~~)~~ is the largest in the Olenekskiy Bay (over 2.5°C), along the coastline close to the ~~Lena river~~ Khatanga estuary (2.5-3°C), the Lena River delta (about 4°C) and in marginal ice zone (mostly over 1.5°C). The remarkable variation of ~~temperature~~ SST in the central part of the Laptev ~~sea~~ Sea should be associated with the thermal fronts (largest SST gradients) displacement.

The averaged SSS is 28.75 ~~PSS~~ in the Laptev ~~sea~~ Sea and 27.74 ~~PSS~~ in the studied part of the East-Siberian ~~sea~~ Sea (Fig. 6). The spatial distribution of mean salinity for ~~August September~~ August-September 2018 has several characteristic features. The freshest ~~waters (~~water (salinity below 20~~PSS~~) are observed within the river plume northeast of the Lena ~~river~~ River delta and within the southern part of the East-Siberian ~~sea. Fresh waters~~ Sea. Water with salinity below 28 ~~PSS~~ reach the sea ice edge ~~on the northeast of the Laptev sea. Additional freshwater~~ in the northeast Laptev Sea. Additional fresher water from the Kara ~~sea~~ Sea enters via the Vilkitskiy and Shokalskiy straits in the west (salinity of 28-30~~PSS~~) and is also observed along the sea ice edge, so it could be associated with ice melting. The most saline ~~waters (~~water (salinity above 34~~PSS) are situated~~) is located in the central part of the Laptev ~~sea~~ Sea near 78-80°N 120-140°E, and in the northwest, along the Severnaya Zemlya Archipelago. As also observed in the SST, the SSS in the Olenekskiy Bay is highly variable, which can be explained by the variation of the freshwater discharge during the 2 months. Nevertheless, large SSS variability is also observed all along the sea ice edge: at 78-80°N in the north and northwest and at the boundary between the Laptev and East-Siberian ~~seas~~Seas. This large variability can be explained in two ways: physical (~~natural~~ haline fronts related to sea ice melting) and instrumental (remaining ice contaminated pixels, lower ~~sensibility~~ sensitivity of L-band in cold ~~waters~~water). At 78-80°N 125°E, free-floating patches of broken ice detached from compact sea ice edge ~~were~~ are observed during several weeks in August-September 2018. Random pieces of broken ice are not always recognized by ice-mask filters, so can artificially increase the SSS variability. At the same time, this is the area where river ~~waters~~ water meet sea ice, which induces natural variability.

3.1 Observed surface water masses of the Laptev Sea and their transformation

To generalise our understanding of vertical structure of the studied area, we use the classical TS-analysis, first based on CTD measurements only. Fig. 7 shows the temperature-salinity distributions in the upper 200 m, where the color of marker indicates depth. The most prominent feature on the diagram is the transformed Atlantic Water mass with salinity close to 34.5-35, temperatures from -0.5 to 2.5 °C lying at a depth of 100-200 m. The water mass overlying the Atlantic Water (between 50 and 100 m depth) is the lower halocline water, described by **?** as having salinity in a range of salinity 33-34.5, and negative temperatures starting from the lowest values presented in Fig. 7, -1.7 to 2.5°C. The surface water observed in the upper 50 metres is in general the less saline (salinity below 34), but one can clearly observe two separate branches with negative and positive temperatures. It should be remembered that a T-S diagram based only on CTD measurements does not provide an instantaneous view on the ocean state, but is a collection of conditions encountered in different regions at different moments of time (from the end of August to the end of September 2018). During the summer months, the surface water of the Arctic Ocean quickly changes its characteristics, and the synoptic satellite data provide an additional information to the point-wise in situ measurements.

Using DMI SST and SMOS SSS weekly estimates, we plotted T-S diagrams similar to that on in Fig.7, but for several reference days: Aug 1, Aug 15, Aug 30, Sept 4, Sept 13, and Sept 30, 2018 (Fig.8). On the lower row, we present all in situ measurements in the upper 6.5 m and the differences between satellite-derived sea surface temperature and salinity of discussed days. It is observed that the DMI SST is rising only up to the end of August with the maximum temperatures from 8 to 11.5°C for some cases, and then decreases to 4.5°C by the end of September. The temperature is changing by 0.5 - 1°C per week (while increasing and decreasing).

Based on the Fig. 8 visual analysis, we propose to identify 6 surface water masses in the Laptev and East-Siberian Seas (Tab.1). The main surface water masses are warm and fresh (WF) river water and cold and saline (CS) open sea water. All other water masses show either different stages of transformation of these two water masses, or are advected from other regions. It should be noted that satellite-derived data have a larger range of temperature and salinity than near-surface (upper 6.5 m) in situ measurements, which makes this detailed classification possible. The locations of the different water masses for selected days are shown in Fig.9 together with the distribution of water masses in percentage (the whole studied area is 100%, and sea ice occupies some part of it).

On August 1, the sea ice still covers more than 80% of the studied area and extends on average to 78°N in the Laptev Sea, while the East-Siberian Sea is almost completely covered by ice. Warm and Fresh (WF) river water is well observable in the south between 74 and 76°N. It occupies almost the same amount of surface as the Cold and Saline sea Water (CS), the rest of the open area is occupied by a transformed river water (Warm and Medium Salinity, WMS, Cold and Medium Salinity, CMS), that already formed a recognisable river plume front: its signature is continuous from 115°E to 150°E up to the northern position of sea ice edge.

During the next two weeks the ice cover retreats, and a Cold and Fresh Water (CF) mass appears in the south-west East-Siberian Sea. The amount of this Water increased progressively in this area during the remaining period. We suggest that this water mass represents the river water trapped under the ice and then exposed.

On the 15th of August, one can notice as well a water mass CMS appearing close to Vilkitskiy Strait. It is less pronounced by the end of August, but a thin stream of cooled and transformed river water from the Kara Sea descends along the Taimyr peninsula in September. The Lena River water mixing and cooling happens as well close to the sea ice edge in the north-east Kara Sea. All in all, the surface occupied by this water mass is steadily growing during the observed period, and is nearly 10% by the end of September. We suggest that water mass CMS is a transformed version of water mass CF.

The end of August is warmer as seen in Fig. 9 with the amount of saline water with temperatures above $3°C$ (water mass WS, Warm and Saline) occupying the central and the western part of the Laptev Sea (almost 10% of the studied area). This water mass is disappearing by the end of September with a decrease of temperature.

By September 13, the SST and SSS variability diminishes. The water mass CF in the north-east Laptev Sea consisting of cold fresh water becomes saltier (transforms into the water mass CMS). The freshwater cools south of the New Siberian island and

Table 1. The temperature and salinity of six defined surface water masses of the Laptev Sea using satellite data (see the text for the explanation of water masses names)

Water mass	WF	WMS	CF	CMS	WS	CS
T	$\geq 3^{\circ}C$	$\geq 3^{\circ}C$	$\leq 3^{\circ}C$	$\leq 3^{\circ}C$	$\geq 3^{\circ}C$	$\leq 3^{\circ}C$
S	≤ 25	$25-29$	≤ 25	$25-29$	≥ 29	≥ 29

by September 25 occupies all the ice-free area. The river plumes signature is shifted to the New Siberian island as well (Fig. 9). Cold and saline water dominates the surface of the Laptev Sea. Finally, by September 25, the T-S diagram shows that most of the points lay between 25 and 35 and -1°C and 4°C, with a main core within a salinity range 25-35 and temperature between -1 to 1°C, and the second one within the salinity range 22.5-30 and temperature of 3-4°C. The Laptev and the East-Siberian Seas start to refreeze, the most rapidly in the areas with cold and fresh river water.

3.2 Freshwater ~~plume extension~~variability in the Laptev Sea

To evaluate the distribution of freshwater input in the Laptev ~~sea during summer months, we considered~~ Sea in August-September 2018, we consider virtual zonal and meridional transects along 78°N and 126°E, respectively~~and plotted their temporal evolution on~~ , and plot the temporal evolution of DMI SST, SMOS SSS "A", wind speed and SLP in Hovmöller diagrams~~(Fig. 10, 12).~~ . The freshwater can be defined by comparison to the saline “marine water” (typically, 34.80 as in **?** or 34.92, as in **?**). As a 0-salinity river water quickly mixes with a saltier marine water, in reality the "freshwater" is more "brackish" than "fresh". Nevertheless, for simplicity assuming a river plume front at the 29 isohaline, the “freshwater” corresponds to all water masses with the salinity lower than 29, as we referred to it in section 3.2.

3.2.1 Water from the Lena River plume

The zonal transect helps to investigate the mean stream position of the river plume away from the coast, in the central part of the Laptev ~~sea~~ Sea with more complex topography ~~.~~ (Fig. 10). This virtual section does not correspond to any real CTD-section, apart from some extracts of TGS profile following the ship’s route (see the position of virtual section on the SST and SSS maps in Fig.10, f-g). In the western part (up to 130 °E), the transect is located roughly above the continental slope and then over the shelf (Fig.~~12). It can be noticed that a displacement of river waters~~ 10, e). The river water displacement roughly follows that of sea ice edge ~~on~~ in the east and is bounded by the ~~edge of the shelf on~~ shelf break in the west. Overall, temperatures are higher in August than in September: a warm pool with SST over 6 °C is observed during the first 30 days at 78°N, 130-147 °E, with highest temperatures on August 26. These coordinates define the position of the river plume at 78°N latitude, as ~~it~~ can be clearly seen in the salinity values varying ~~from~~ in a range of 27-30 ~~PSS~~ there. Relatively strong daily winds (10-12 m/s) observed during the first 10 days of September ~~are~~ were associated with a ~~passage of~~ series of cyclones~~and strongly impact~~ , which strongly impacted the surface layer: the median temperature over the zonal transect ~~decreases~~ decreased from 3°C to almost 0°C, and salinity ~~changes by 1 PSS.~~ increased by 1. As the amount of incoming solar radiation diminishes in

September, the maximum SST values ~~do not overpass~~ did not exceed 3°C anymore. Nevertheless, ~~in~~ at the end of September a new freshwater patch ~~is seen~~ was observed at 140°E (less ~~observed~~ visible in SST field) indicating that the ~~surface mixed layer~~ "upstream" surface mixed layer (in the southern part of the Laptev ~~sea) contains~~ Sea) contained a sufficient amount of freshwater to restore its previous state after a mixing event ~~.~~ induced by the wind. Another possible explanation is that a small peak observed in the Lena River discharge in the first days of September (Fig.3) helped to introduce an additional portion of freshwater that reached 78°N several weeks later.

3.2.2 Water from the Kara ~~sea waters~~Sea

~~Zonal~~

The zonal transect allows to see not only the Lena ~~river~~ River plume, but ~~to observe~~ as well the Kara water intrusions ~~on the West. Selected~~ in the west. The selected zonal transect at 78°N is partly ~~laying~~ lying above the Vilkitskiy Strait connecting the Kara and the Laptev ~~seas. In salinity fields of the zonal Hovmöller diagram, we~~ Seas. Being a reservoir for two other great Siberian Rivers, the Ob' and the Yenisei, the Kara Sea has a low salinity compared to the central Arctic Basin (**?**). In the absence of significant river sources on the Severnaya Zemlya Archipelago, we considered that the freshwater input close to the Vilkitskiy and the Shokalsky Straits arrived from the Kara Sea.

We observe the freshwater arriving from the Kara ~~sea~~ Sea at 110-115°E with typical values of 25-28 ~~PSS~~ during the first 20 days of August and ~~in~~ at the end of September ~~. It is remarkable, that~~ (Fig.10, b). It is noteworthy that the SST fields do not indicate the presence of these intrusions ~~in such clearlyway. It might be possible, that fresh waters~~ so clearly. This suggests that fresh and warm water of the Ob' and Yenisei rivers arriving to the Laptev ~~sea~~ Sea have already lost a significant part of their heat content via exchange with the atmosphere, but ~~the fresh water layer wasn't~~ that the freshwater layer is not completely mixed with the surrounding sea environment. ~~The~~

In Fig. 11, the CTD data justify that the amount of ~~fresh water~~ freshwater arriving from the Kara ~~sea via Vilkitskiy strait is significantly higher than that one~~ Sea via Vilkitskiy Strait is significantly greater than freshwater arriving via the narrow and rather shallow (250 m) Shokalskiy Strait between the Bolshevik and the October Revolution Islands or ~~northward~~ north of the Severnaya Zemlya ~~archipelago~~ Archipelago at the traverse ~~of~~ near the Arkticheskiy Cape across the continental slope~~(Fig. ??).~~ . The temperature of the surface layer is increasing ~~from the North to the South from~~ between 0°C to 3.5°C from the North to the South. The salinity sections indicate the ~~freshwaters~~ freshwater with salinity above 29 ~~PSS~~ only in the Shokalskiy and the Vilkitskiy straits, which suggests ~~the very low~~ very little advection of the Kara-origin ~~fresh waters by~~ freshwater via the north. From the buoyancy cross-sections, one can find that the strongest stratification is at 5-20 m depth, which corresponds to the 1024-1025 kg/m^3 isopycnals position. This result argues against a definition of fresh-water content by the 1027.35 kg/m^3 isopycnal of **?**, as the surface salinity and temperature in the Siberian shelf seas are lower than in other regions. ~~The definition of fresh water content in the Arctic might be considered again.~~

3.2.3 Meridional transect

The meridional transect along 126°E (Fig. 12) partly corresponds to the standard oceanographic section 5 carried out during ARKTIKA-2018 expedition on September 1-4, 2018 (Fig.13). This transect helps to understand the northward propagation of the river plume and to evaluate the freshwater content using in situ data. The highest ~~temperature observed at this~~ SST observed along 126°E longitude is 8°C in August (please note, that a small cold temperature intrusion on days 22-26 ~~most likely corresponds to the~~ probably corresponds to an error in DMI ~~L4~~ SST product due to a cyclone passage ~~, which is seen on~~ and thus, either bad cloud masking or strong winds. This is an assumption reinforced when comparing DMI ~~to~~ SST to SST AMSR2 microwave data (not shown here). More information on the SST corrections in Arctic can be found in the work of **?**).

The warmest ~~and freshest waters of river plume occupy~~ (5-9°C) and freshest (salinity of 20-30) water of river plume occupies the area between 74-77°N in August and progressively ~~retreat~~ retreats in September: SST and SSS gradients become wider and less pronounced, temperature decreases to 3-4 degrees. High ~~winds~~ wind speed (10-12 m/s) associated with ~~a depression~~ an atmospheric cyclone passage during the first two weeks of September ~~are seen~~ is found both on the meridional and the zonal ~~Hövmoller~~ Hovmöller diagrams and might ~~be related to~~ explain this widening of the surface thermal and haline frontal area. Nevertheless, a point-wise cross-correlation between the time-series of wind speed and temperature or wind speed and salinity in a point with random coordinates does not give statistically significant results: both correlation coefficients are below 0.2 ~~with~~ at any time lag (0-10 days). Better correlation is observed with sea level pressure (up to 0.6 at some points), but over the 56 days of the studied period it is not statistically representative as only two passages of cyclone were observed. ~~Higher values of cross-correlation coefficient are expected over the frontal zone, as this is the area exposed to rapid changes.~~

~~Oceanographic~~ The oceanographic sections allow to estimate a thickness of the freshwater layer and how far the river water propagates under the ice. Section 5 provides a complementary information to the meridional Hovmöller diagram (Fig.13, upper row) as it was done along the same 126°E parallel from 76 to 81.4° N on September 1-4 2018. This ~~moment~~ date corresponds to the passage of several cyclones over the Laptev ~~sea~~Sea, which, in turn, displaced the river front to the south, unfortunately, almost ~~out of scope of~~ away from this oceanographic section. Nevertheless, at 76-78° N (first 200 km of the section), ~~the low salinity~~ low salinity between 29-33 ~~PSS~~ was still observed in the upper 25 meters. A thin upper layer with positive temperatures has the same thickness, but ~~vasts~~ extends further northward, up to 79° N. ~~On~~ In the north of the section, under the ice, the temperatures are below 0°C and salinity is rather low, below ~~32 PSS.~~ 32. The low salinity under the ice ~~can indicate~~ suggests that the residuals of the river ~~waters~~ water arrived in this area earlier. If the river ~~waters~~ water were propagating under the ice when the Laptev ~~sea~~ Sea was not yet completely open, ~~one~~ we should assume their further mixing with sea ~~waters~~ water when the sea started to open in its central part (mixed ~~waters~~ water with salinity between 30 and 32 ~~PSS~~ and still positive temperatures). The heat exchange with the sea ice might be more effective than with the atmosphere, so under the ice the temperatures are negative, and river water signal is not observed anymore, contrary to salinity. At the same time, it depends on thermal conductivity in the ice, and its initial temperature profile, so this question needs a special attention.

Overall, the first 150 km over the shelf, where the warmest and freshest ~~waters~~ water were observed, are characterized by the strongest stratification in the upper 25 m layer. This is the depth of a stable stratification for the whole section, though

~~less pronounced~~ stratification is less pronounced in the deeper part of the sea than over the shelf. Below the pycnocline, one can observe cold (with negative temperatures) and saline (salinity between 33 and 34.5~~PSS~~) water mass. The warm ~~and saline Atlantic water~~ (T above 0°C, following **?**) and saline (S above 34) Atlantic Water spreading along the continental shelf is best identified in temperature vertical profiles at 100-120 m depth, but is also detected by the instability signal (right column ~~on~~ in Fig. 13). The propagation of the Atlantic ~~waters in laying~~ Water is beyond the scope of this paper, and though Atlantic Water is observed in all ~~discussed below oceanographic sections~~ oceanographic sections presented below, it won't be ~~presented~~ discussed furthermore.

When considering other meridional sections (section 6, 8, and 7 according to their positions from the west to the east), one can follow the eastward propagation of the river ~~waters away from their origin, the Lena river~~ water away from the Lena River delta. Section 6 started on September 5 in the vicinity of the marginal ice zone ~~on~~ in the deep North-Eastern part of the Laptev ~~sea~~ Sea and ended in the ice-covered part of the East-Siberian ~~sea~~ Sea over the shelf on September 9. This section is not exactly perpendicular to the continental slope, so we can not estimate the width of the river ~~waters~~ water plume, but overall the thickness of the upper layer is similar ~~to that one~~ (20-30 m) to that observed with section 5 in the deep part of the section~~(20-30 m). The waters~~. The water over the shallowest part (depth smaller than 60 m) were observed under the ice, ~~which~~ as is clearly seen in the temperature signal that is negative even close to the surface. At the same time, the main freshwater core with the highest temperature is observed above the shelf break. The second core is observed in the northern part of the section, with lower salinity than ~~on~~ in the north of section 5. The mixing over the shelf was effective enough to stretch the isopycnals ~~in the vertical up from the surfaceto the bottom~~between the bottom and the surface. Nevertheless, the depth of the maximum stratification is close to 20 ~~meters~~ metres as for the shallow part of the section 5. Over the edge of the continental slope, the maximum ~~value of~~ Brünt-Väisälä frequency ~~is deepen~~ moved deeper to 25 m, and over the deep-water part to 30 m depth.

Section 8 was started on September 15 in MIZ over the deep part of the East-Siberian ~~sea~~ Sea and finished by September 17 in the ~~free of ice~~ ice-free area over the shelf. The river signal is still very pronounced ~~in both temperature and~~ both in temperature and in salinity profiles, with an efficient mixing over the 60 m layer ~~at~~ on the shelf and more ~~condensed~~ concentrated isopycnals over the shelf edge. The most eastern section 7 was conducted under the ice. The temperatures are, thus, negative above the Atlantic ~~water~~Water, but salinity profile reveals the river water presence with the freshwater core having salinity below ~~29 PSS.~~ 29. The maximum value of Brünt-Väisälä frequency are ~~lower~~ less than for other sections and are observed at 20 m depth and at 55 m depth, following 1024 kg/m^3 and 1026.5 kg/m^3 isopycnals, accordingly.

To ~~resume, in~~ summarize, during the summer 2018, we observe a north-eastern displacement of the Lena ~~river waters~~ River water including in the MIZ and ice-covered area. We suggest that the active displacement started in the ice-covered conditions after the maximum of river discharge in ~~July~~ June-July (following the **?** study and the Lena River discharge measurements presented in Fig.3), then, with progressive opening, a part of the river ~~waters~~ water was mixed within the upper ~~layer of sea and exchanged the~~ sea layer and exchanged heat with the atmosphere. Regarding the ~~waters~~ water under the ice, the heat flux from the river water to the sea ice resulted in cooling of ~~the latter~~ these water to the ambient negative temperature, but, at the same time, the sea ice protected the freshwater layer from wind-induced mixing, so it conserved a pronounced ~~signal in salinity~~salinity signal.

3.2.4 Tracing surface water origin using oxygen isotopes (delta-O18)

The oxygen isotopes are considered as a "natural tracer of river runoff in the Arctic Ocean" (**?**) and are widely used to detect the origin of water masses (**?**, **?**, **?**). The most simple approach to detect a river water fraction in a water sample is to compute a ratio between the measured salinity and oxygen isotope 18 (delta-O18). As it was described in Data and Methods Section, we used only the surface measurements in the upper 3 m layer.

Using a rather simple three-component model to distinguish the marine water, the river water (meteoric water), and the sea ice melt water described in **?**, we calculated the fractions of each water (Fig. 14). In the work of **?**, authors provide values of end-members of this model (typical salinity for each water mass and typical d-O18 concentrations), so after resolving a simple system of three linear equations using the values of the total (measured) salinity and the measured d-O18 concentration, we found a contribution of each fraction. As done in **?**, the role of precipitation is neglected in this model, as its amount is insignificant compared to the river water input. The sea ice melt fraction can be negative in case of sea ice formation.

3.2.5 ~~Mean monthly observations.~~

~~In aprevious study on~~ This analysis indicates that the most important fraction of river water is brought over the shelf and the shelf edge of the East-Siberian Sea (Fig.14, a). At the same time, the water samples at the northern part of the 126°E section consist of 10-15 % of the river water and only of 0-5% of the sea ice melt fraction. Knowing that the main maximum of the river discharge occurs in June (Fig.3), this fact supports our hypothesis that a noticeable amount of river water was distributed under the ice far northward into the deep part of the Laptev Sea (north of 80.5°N), where it will enter the central Arctic Basin later. It is interesting that the areas with the highest sea ice melt fraction (Fig.14, c) (5-10%) very slowly follow the sea edge, so they were observed in the central and western part of the Laptev sea and in the MIZ area in the East-Siberian Sea. The sea ice formation (the negative values of sea ice melt fraction) is found in MIZ and its vicinity at 78-70°N - 150-150°E of the East-Siberian Sea. The presence of river waters may accelerate the sea ice formation if the air temperature favours it. The surface water samples of the western and central parts of the Laptev sea consist of large marine water fraction (90-95%). The lowest marine water fraction (75-80%) was found over a very shallow ice-free area between the New-Siberian islands and MIZ in the East-Siberian Sea, where both sea ice melt and river water fractions are relatively high (5-10% and 10-25% respectively). Actually, it is the area of the most intense surface mixing that was observed using in situ measurements during the ARKTIKA-2018 expedition.

3.3 Wind forcing.

A previous study in this region (**?**) claimed that the surface fronts displacement is mainly governed by the wind and atmospheric pressure centers. To investigate ~~it, we computed mean wind fields and the~~ the role of the wind forcing at the synoptic scales, we compute mean monthly Ekman transport for August and September 2018 (Fig. 15). ~~Horizontal transport was calculated for the first meter as:~~ The calculation is described in the section 2.

$$u_{ekm} = \frac{\tau_v}{\rho_w * f}$$

$$v_{ekm} = -\frac{\tau_u}{\rho_w * f}$$

where u_{ekm} and v_{ekm} are horizontal components of the Ekman transport, τ is a wind stress, calculated from ASCAT winds (u_{wind}, v_{wind}) using ERA5 air density ρ_{air}: $\tau_u = C_D * (u_{wind}) * u_{wind} * \rho_{air}$; ρ_w is a surface density, calculated from The discussed displacement of the river plume extension in August and September are well seen in both SST and SSS with TEOS-2010; C_D is surface drag coefficient calculated from wind speed according to ?, f is the Coriolis parameter.

Vertical Ekman speed (upwelling and downwelling)was computed as:

$$w_{ekm} = \frac{1}{\rho_w * f}\left(\frac{d\tau_v}{dx} - \frac{d\tau_u}{dy}\right) + \frac{\beta * \tau_u}{\rho_w * f^2}$$

where w_{ekm} is a vertical component of the Ekman transport and β is a beta-plane approximation of the Coriolis parameter.

The mean monthly fields (Fig.15 a, d and b, e, respectively). The most pronounced feature in the SST field is the drop of SST by 3°C in the central and southern part of the Laptev Sea. The salinification of the northern, central, and southwestern part is observed in August-September SSS fields. The average wind speeds were are low to moderate during two discussed summer monthsAugust and September, 3-7 m/s . (Fig.15 c, f). The wind field in August was is more homogeneous and velocities are slightly higher with general south-eastern an overall south-easterly direction; the Ekman transport pushed pushes the river water out of the central part of the Laptev Sea favouring its propagation under the ice. A large area of convergence and downwelling is seen eastward to east of the Taimyr peninsula at 77°N 120°E. Almost the rest of the studied area is an upwelling zone, with large values of vertical velocity in the Vilkitskiy Strait and following the river front above the continental slope in the central part of the Laptev seaSea.

In September, the wind changed changes its main direction to the south-western, which led to south-westerly, which leads to a river water blocking in the Yanskiy bay, still favouring the freshwater flux propagation under the ice, but mostly into the southern part of the East-Siberian Sea. A large-scale divergence and upwelling on the North-West of the Laptev sea in the north-west Laptev Sea was observed as well. The Ekman vertical velocities in September differed differ from August. Several downwelling zones were are observed: in front of the Lena delta, close to MIZ on the North-Eastin the north-east, and in the deep part of the central Laptev seaSea. The irregular pattern of the upwelling and downwelling facilitate the mixing of different water masses, which is more active, thus, in September.

4 Observed water masses of the Laptev sea

To generalise our understanding of vertical structure of the studied area, we used the classical TS-analysis, first based on CTD measurements only. Fig. 7 shows the temperature-salinity distributions in the upper 200 m, where the color of marker indicates depth. The most prominent feature on the diagram is the transformed Atlantic water mass with salinity close to 34.5-35 PSS, temperatures from -0.5 to 2.5 °C laying at a depth of 100-200 m. The water mass overlaying the Atlantic water (between 50 and 100 m depth) is the lower halocline water, described by **?** as having salinity in a range 33-34.5 PSS, and negative temperatures starting from the lowest values presented on Fig. 7, -1.7 to 2.5°C. The surface water observed in the upper 50 meters is in general the less saline (below 34 PSS), but one can clearly observe two separate branches with negative and positive temperatures. It should be remembered that TS-diagram based only on CTD measurements does not provide an instantaneous view on the ocean state, but is a collection of sea states in different regions at different moments of time (from the end of August to the end of September 2018). During summer months, the Arctic ocean waters quickly change their characteristics, and satellite data provide additional information to the pointwise in situ measurements.

TS diagram based on the CTD data in the upper 200 m

Using

4 Discussion and conclusion

Based on in situ and satellite measurements, we document the evolution of the water masses during August and September in the Laptev and the East-Siberian Seas. Satellite DMI SST and SMOS SSS weekly estimates , we plotted T-S diagrams similar to that on on Fig.7, but for several reference days: Aug 1, Aug 15, Aug 30, Sept 4, Sept 13, and Sept 30, 2018 (Fig.8). On the lower row, we present all in situ measurements in the upper 6.5 m and the differences between satellite derived temperature and salinity of discussed days. It is clearly seen that the SST is growing only up to the end of August with the maximum temperatures from 8 to 11.5$°C$ for some case, and then decreases to 4.5 $°C$ by the end of September. The temperature is changing by 0.5 - 1 degree per week (while increasing and decreasing).

Based on the Fig. 8 visual analysis, we propose to identify 6 surface water masses "A" estimates are cross-validated with continuous TSG measurements and CTD data (rarely done in this region). For the first time, we follow how the river water input is distributed and where it is stored in the Laptev and the East-Siberian seas (Tab. 1). The "classical" water masses are warm and fresh river waters ("1")and cold and saline open sea waters ("6"). All other water masses shows different stages of transformation of these two, either water masses advected from other regions. It should be noted that Sea at synoptic scale. It became possible thanks to new satellite-derived data have a larger range than surface salinity field (SMOS SSS "A"), a vast range of in situ measurements , which makes this detailed classification possible. Positions of defined water massesfor selected days are shown on Fig.9 together with the distribution of and also results of geochemical analysis.

To investigate local surface water masses, a variation of a classical TS analysis is studied using satellite measurements. It helped to define new surface water masses adapted for the Eastern Arctic Ocean with typically low salinity and discuss their transformation. As the validity of SMOS SSS was demonstrated successfully and SMOS measurements are accessible from 2010 to the present, this technique could be applied for the future studies of surface water masses in percentage (the whole studied area is 100% and sea ice occupies some part). transformation at different time scales.

On August 1, the sea ice covers yet more than 80% of the studied area and extends in average to 78N in the Laptev sea, while the East-Siberian Sea is covered almost completely. Warm and fresh river water ("1") is well observable on the South up between 74 and 76N. It occupies almost the same amount of surface as cold and saline sea water ("6"), the rest of the open area is a transformed river water (”2”, ”4”), that forms already a recognisable river front: its signature is continuous from 115E to 150E up to the northern position of sea edge. In two weeks the ice cover retreats, and a fresh and cold water ("3") mass appear on the south-west of the East-Siberian sea. The amount of this waters will increase progressively in this area during the rest period. We suggest that this water mass represents the river waters captured under the ice and then exposed back.On the 15th of August, one can notice as well a water mass "4" appearing close to Vilkitskiy Strait. It is less pronounced in the end of August, but a thin stream of cooled and transformed river waters from the Kara sea descends along the Taimyr peninsula in The transformation of fresh river water input occurs very quickly during the Arctic summer, of the order of 1-2 weeks. Our observations suggest that the vertical mixing, a weaker river discharge, and a continuously decreasing radiative income impact the variability of surface water characteristics, as is particularly well seen in the beginning of September. The Lena river waters mixing and cooling happens as well close to the sea ice edge on the north-east of the Kara sea. All in all, the surface occupied by this water mass is steadily growing during the observed period, and is around 10% by the end of September. One can imagine that water mass "4" is a transformed version of water mass "3".

The end on Augustis the warmest, it is seen at Fig. 9 with the amount of saline waters with temperatures above $3°C$ (water mass "5") occupying the central and the western part of the Laptev sea (almost 10% of the studied area). This water mass is disappearing by the end of September with a decrease of temperature. By September13, the SST and SSS variability slow down. The water mass "3" on the north-east second yearly maximum of river discharge occurs in the beginning of August. The warm and fresh river water is redistributed and transformed in the surface layer of the Laptev Sea during the month of August, but after the passage of several cyclones in the beginning of September, there is no additional important source of heat and fresh water that would maintain the variability of water masses. Globally, in September, the water mass CS progressively occupies the ice-free surface of the Laptev sea consisting of cold fresh water becomes saltier (transforms into the water mass "4") . The fresh water cools on the south to the New Siberian island and by September 25 occupies all the area free of ice. The river plumes signature is shifted to the New Siberian island as well (Fig. 9). Saline and cold water mainly dominates the surface of the Laptev Sea. Finally, by September 25, instead of other (“transformed”) water masses observed there in August. The ice formation starts at the end of September and sea surface will be covered by November, so it seems that freezing will begin only after the heat accumulated during the summer season is released to the T-S diagram shows that most of the points lay between 25 and 35 PSS and -1°C and 4°C, with a main core within a range 25-35 PSS and -1 - 1C. The Laptev and the East-Siberian seas start to refreeze, the most rapidly in the area with cold and fresh river waters. atmosphere and the water temperature at the surface drops to the freezing point.

Surface water masses Water mass 1 2 3 4 5 6T $> 3C$ $> 3C$ $< 3C$ $< 3C$ $> 3C$ $< 3C$S $< 25PSS$ $25 - 29PSS$ $< 25PSS$ $25 - 29PSS$ $> 29PSS$ $> 29PSS$

Temporal evolution of surface water masses in August-September 2018 for the following reference days (upper row): Aug 1, Aug 15, Aug 30, Sept 4, Sept 13, and Sept 30, 2018. Color represents the density of points (number of observations with this temperature and salinity). Lower row: T-S diagram based on CTD measurements in the upper 6.5 m only, and the differences (in density points) between the reference days.

~~Water masses spatial distribution in August-September 2018: upper row - Aug 1, Aug 15, Aug 30; lower row - Sept 4, Sept 13, Sept 30. Sea ice cover from AMSR2 is plotted as dashed area.~~

~~In this work, we discussed the water masses evolution in the summertime in the Laptev and the East-Siberian seas. The cross-validation of satellite-derived SST L4 distributed by DMI was done with continuous TSG measurements. For the first time the capacity of SMOS to follow a temporal evolution of the Lena river plume in the Laptev sea under influence of atmospheric forcing was demonstrated.~~ A pathway of the low salinity Kara ~~waters was~~ water is observed during several days of ~~the studied period. Kara waters propagated~~ study. The Kara water propagates mostly through the Vilkitskiy Strait and partly through the Shokalskiy Strait, but no freshwater ~~was~~ is found northward of the Severnaya Zemlya Archipelago. ~~Pursuing~~ Propagating along the coastline, ~~this low salinity water arrives into~~ the low-salinity Kara water enters the Oleneksiy bay where it meets another freshwater flux from the ~~Lena and Khatanga rivers.The~~ Khatanga and the Lena rivers. The arrival of freshwater via the Vilkitsiy Strait was already studied using in situ data by **?**, **?**, this is the first time this event has been observed from satellite data which provide a unique regular monitoring. The freshwater input from the glaciers and icebergs of the Severnaya Zemlya Archipelago should probably also be taken into account, but this is out of scope of this study, and we assume this source of freshwater as negligible compared to the very fresh Kara Sea water.

The wind situation in August was favorable for the extreme propagation of river ~~waters into the central and the~~ water into the north-eastern part of the Laptev ~~sea~~ Sea with following penetration into the East-Siberian ~~sea~~ Sea in MIZ and under the sea ice. The ~~fresh waters displacement should be associated with the Ekman transport. We claim as well~~ propagation of river water under the sea ice is apparent in the western part of the East-Siberian Sea, where two branches with warm and fresh cores were observed with in situ data.

The Ekman transport illustrate a possible forcing for the freshwater displacement. As the theoretical Ekman depth is controlled mainly by the Coriolis parameter f (and also by viscosity), in the south of the Laptev and the East-Siberian Seas it exceeds the depth of some shallowest areas (according to **?** study in the same region the Ekman depth is $D_{Ekm} = 37$ m: see the position of 37-m isobath in the Laptev Sea in Fig.15). Thus, the calculated Ekman transport should be regarded as a theoretical concept illustrating possible mechanisms of horizontal transport and vertical mixing in the central and northern areas. A new sea level dataset provided by DTU for the Arctic Ocean and calculated geostrophic currents, discussed in the Appendix, enriches the overview of the surface ocean dynamics during selected summer months.

On a larger scale, this situation can be also explained by a positive (in April-October 2018) Arctic Oscillation index favoring the eastward propagation of fresh water, as it was demonstrated in works of **?**, **?**, **?**. An important part of the northward propagation to the shelf edge is not explained by the positive AO. Based on the oxygen isotopes results, we claim that a similar propagation of river ~~waters far to the North~~ water far northward happened before the observed period (in June-July), when the Laptev ~~sea~~ Sea was still covered with ice and the Lena ~~river discharge was supposed to be the maximum (following the results of ?). On~~ River discharge was the largest (Fig.3). In the north of the 126°E section, under the ice, the upper 25-m layer is ~~freshen to~~ fresher with a salinity below 33~~PSS~~, which supports this hypothesis~~; and there~~. There is no evidence that the sea ice melting itself can create such a considerable layer of freshwater. Our isotopes estimates could be refined using alkalinity to separate the meteoric water estimated with water isotopic analysis (river input from precipitation).

A study of **?** ~~defend the hypothesis of river waters, as~~ also supports the influence of river water, as a similar situation was observed in 2011. Unfortunately, the present spatial resolution of satellite-derived SSS and its uncertainty due to the ice proximity ~~make~~ makes it difficult to separate river water from the freshening associated with the sea ice melting~~from river waters. No direct measurements~~. No accurate satellite measurement of sea ice thickness ~~were carried out in this region at this moment of time neither~~in MIZ exists at present to the best of our knowledge, so it is complicated to evaluate the freshwater input due to the sea ice melting ~~only. The propagation of river waters under the sea ice is apparent in the western part of~~ on the scale of several months. Nevertheless, the ~~East-Siberian sea, where two brunches with warm and fresh cores were observed with in situ data. In September, we illustrated the processes of rapid autumn cooling of the surface waters in the Laptev sea associated with a series pf atmospheric depressions. Calculated monthly Ekman pumping indicates the area of most intense mixing processes. A new sea level dataset provided by DTU for the Arctic ocean and calculated geostrophic currents, discussed in the Appendix, enriches the overview of the surface ocean dynamics during selected summer months.To generalise the evolution of surface water masses, a variation of a classical TS analysis was proposed using satellite measurements. It helped to define new surface water masses adapted for the Arctic ocean with typically low salinity . As the validity of SMOS SSS was demonstrated successfully and SMOS measurements are accessible from 2010 to the present moment, this technique can be applied for further interannual analysis of surface water transformation~~existing satellite data already have a great potential for the Arctic studies of fresh water. To improve our evaluation of the freshwater budget in the Arctic Ocean, we suggest that appropriate numerical models assimilate the estimates of river discharge, new satellite-derived sea surface salinity and wind data.

Appendix A: Altimetry and geostrophic currents

Two monthly fields of absolute dynamic topography (ADT) and geostrophic currents were calculated from sea level anomalies (SLA) Arctic L4 product and mean dynamic topography (MDT) provided by Danish technological University (Fig. A1). Sea level anomalies are available as mean monthly values on ~~an~~ a grid adapted to polar regions ~~grid~~ with 0.25°step for latitudes, and 0.5°step for longitudes. Mean dynamic topography global one-minute model was used to compute ADT. The resulting monthly absolute dynamic topography ($ADT = MDT + SLA$) was calculated for selected summer months.

Overall, the ADT ~~follows remarkably~~ remarkably follows the ocean bottom topography with higher SLA over the shelf and lower SLA over the deep part of the studied area, which corresponds to the study of **?**. The only exception is negative SLA in the Olenekskiy bay in August 2018. We suggest that the general northward wind-induced displacement of the ~~waters~~ water over the very shallow southern part of the sea was compensated only by the river ~~waters~~ water inflow to the east of 122°E, close to the Lena ~~river~~ River delta. Positive SLA were more pronounced in September than in August, though in August the SST was higher over the southern and central part of the Laptev ~~sea~~Sea, and the salinity was lower in the Olenekskiy bay. The importance of sterical component in variation of the sea level in August-September is ~~, thus , doubtable,~~ thus doubtful, though several source of uncertainty can impact the quality of provided SLA data: uncertainty in tidal model, bathymetry precision, accuracy of the MDT over the shallow part of the Laptev ~~sea, etc~~Sea, etc, as **?** noticed in his work. It should be noted that SSH of the Laptev and the East-Siberian Seas presented in the work of **?**, had the lowest correlation with in situ gauge measurements in the Arctic Ocean, because of the "seasonal runoff".

The geostrophic currents were calculated following classical formula: $u_g = \frac{-g}{f}\frac{dh}{dy}$, $v_g = \frac{g}{f}\frac{dh}{dx}$, where h is ADT, x and y are the distance in ~~meters~~metres. Geostrophic currents presented ~~on~~ in Fig.A1 are very weak and demonstrate rather chaotic structures during selected months. Among the well-pronounced features, an outflow from the Laptev ~~sea~~ Sea in the Vilkitskiy ~~strait~~ Strait is noticeable. Above the continental slope edge, the principal direction of currents is ~~the eastern~~ westward with a maximum current speed of 0.5 m/s. ~~On~~ In the south, an outflow at 122 °E and 130°E ~~helps to bring the Lena waters~~ contributes to transport the Lena River Water into the central part of the Laptev ~~sea~~Sea. In the Yanskiy bay a vortex-like system exists in both ~~,~~ August and September 2018. Geostrophic currents in the East-Siberian ~~sea~~ Sea were calculated from the altimetric measurements in MIZ, so should be interpreted with care. ~~A~~ **?** stated that the SSH measurements there cannot reflect the mesoscale phenomena, because of the small Rossby radius (of order 1 km) and the altimeter along-track resolution of 300 m. At the same time, the same study reported the largest eddy kinetic energy in the shallowest areas.
From our calculations, a cyclonic feature of 150 km in diameter is seen at 79°N, 157°E, and might be topographically induced, as well as a similar cyclonic feature at 78.5°N 135°E. An extended study should be carried out to validate the accuracy of altimetry-derived currents in this region with mooring or vessel mounted ADCP measurements.

Competing interests. No competing interests are present

Acknowledgements. We thank Jean-Luc Vergely for fruitful discussions about SMOS SSS data filtering in the Arctic ocean. We thank Mattew Alkire, Andrey Novikhin, Natalia Vyazigina, all hydrochemistry team of the ARKTIKA-2018 expedition and Ekaterina Chernyavskaya for the collection of water samples for the oxygen isotopes analysis, their analysis and further discussion. We thank all the scientific team of the ARKTIKA-2018 expedition and the crew of RV Akademic Tryoshnikov for their work. This study was supported by the French CNES-TOSCA SMOS-OCEAN project. Anastasiia Tarasenko, Vladimir Ivanov and Nikita Kusse-Tiuz ~~acknowledges~~ acknowledge financial support from the Ministry of Science and Higher Education of the Russian Federation, project RFMEFI61617X0076.

Sea surface temperature validation: example of DMI SST L4 image for September 13 (upper left) with the provided error estimates (upper right); comparison of collocated SST and in situ data in the upper 6.5 m (lower left) and distribution of error provided by DMI and absolute difference measured from comparison with in situ data (lower right)

3.1.1 Salinity

In this section, we compare SMOS SSS relative to in situ measurements. Figure 5 presents the SMOS SSS. We carry a collocation of SSS and in situ measurements of salinity in the upper 6.5 m layer, similar to that one for the temperature described above, except that the averaging of the TSG salinity was done over one hour period (equal to ~ 15 km distance) in order to be closer to SMOS resolution. Comparison between SMOS retrieved error and error based on comparison with cruise salinity measurements is presented on Fig. 5. It shows a good agreement between distribution of SMOS SSS weekly error estimated from retrieval process and distribution of error obtained from comparison with Akademik Tryoshnikov salinity measurements. This results allow us to use SMOS error with a higher confidence in our further analysis. Take into account the SMOS error makes possible to increase the quality of the comparison between the SMOS SSS and the vessel SSS. Using error filtering points too close to the ice edge are excluded. We used 985 collocated points. Comparison between the in situ salinity and SMOS post-processed SSS shows a very good agreement, not yet demonstrated before by any other salinity product in the Laptev sea. The correlation coefficient is 0.86 with a RMS = 0.86 PSS. The bias is 2.06 PSS. For the further analysis we subtracted this bias from the entire SMOS SSS dataset. Standard deviation of SMOS SSS with respect to in situ SSS do not depend on the depth of in situ salinity measurements above 6.5 m, either because in situ salinity is homogeneous vertically or because comparisons are too noisy to detect this small variations (not shown). Although SMOS shows a good agreement most of the time, some larger error can occur close to the ice margin or when pixels are contaminated by small ice pattern that are not detected by AMSR2 sea ice concentration (as observe at 125E and 80N on 5 top, left).

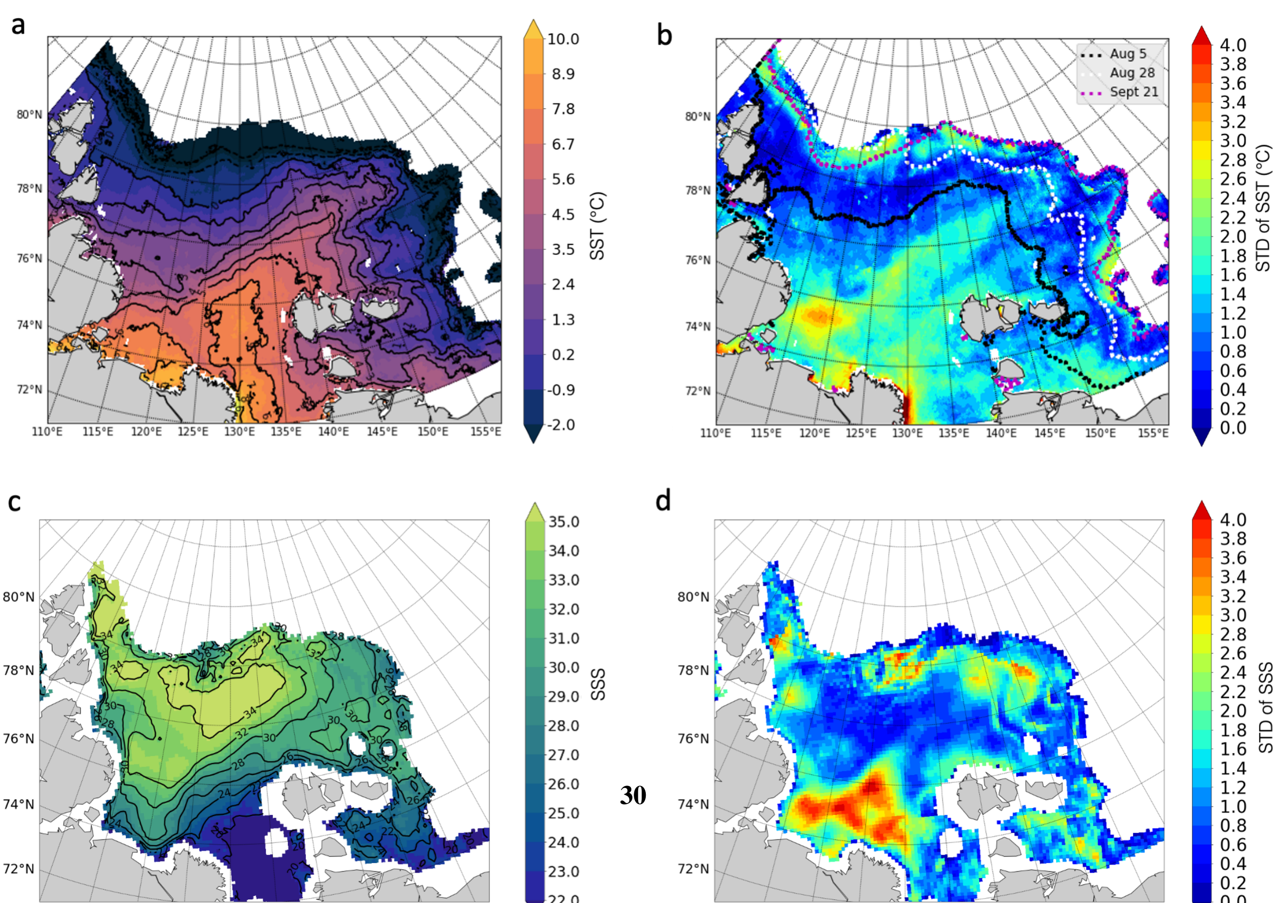

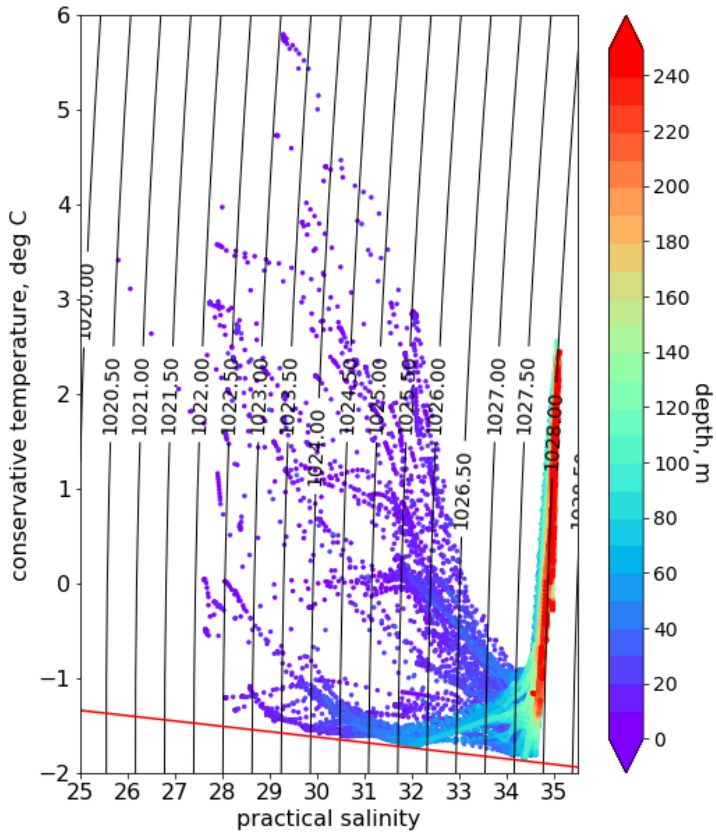

Figure 7. ~~Mean DMI SST (~~T-S diagram based on the CTD data in the upper ~~row) and SMOS SSS (lower row) ~~250 m. Depth of each measurement is shown with ~~their standard deviation for August-September 2018~~color. Red line shows the freezing point.

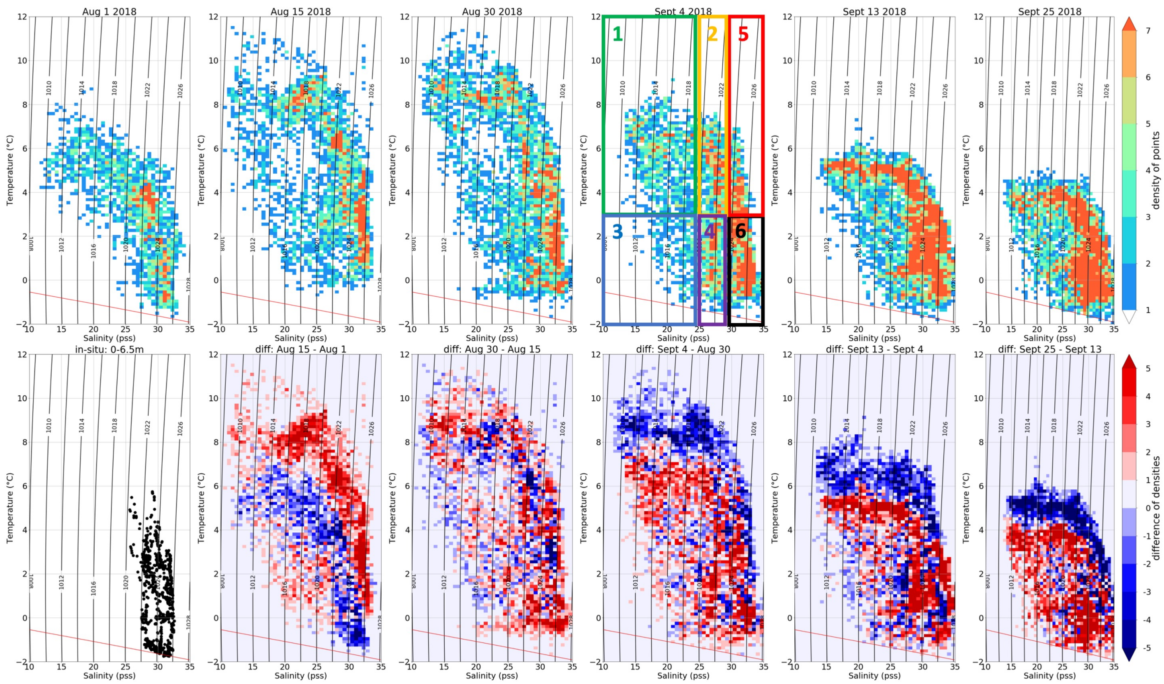

Figure 8. Temporal evolution of surface water masses in August-September 2018 for the following reference days (upper row): Aug 1, Aug 15, Aug 30, Sept 4, Sept 13, and Sept 30, 2018. Color represents the density of points (number of observations with this temperature and salinity). Red line shows the freezing point temperature for different salinity. The boxes show the cores of 6 water masses described in text: 1 - WF, 2 - WMS, 3 - CF, 4 - CMS, 5 - WS, 6 - CS. Lower row: T-S diagram based on CTD measurements in the upper 6.5 m only, and the differences (in density points) between the reference days.

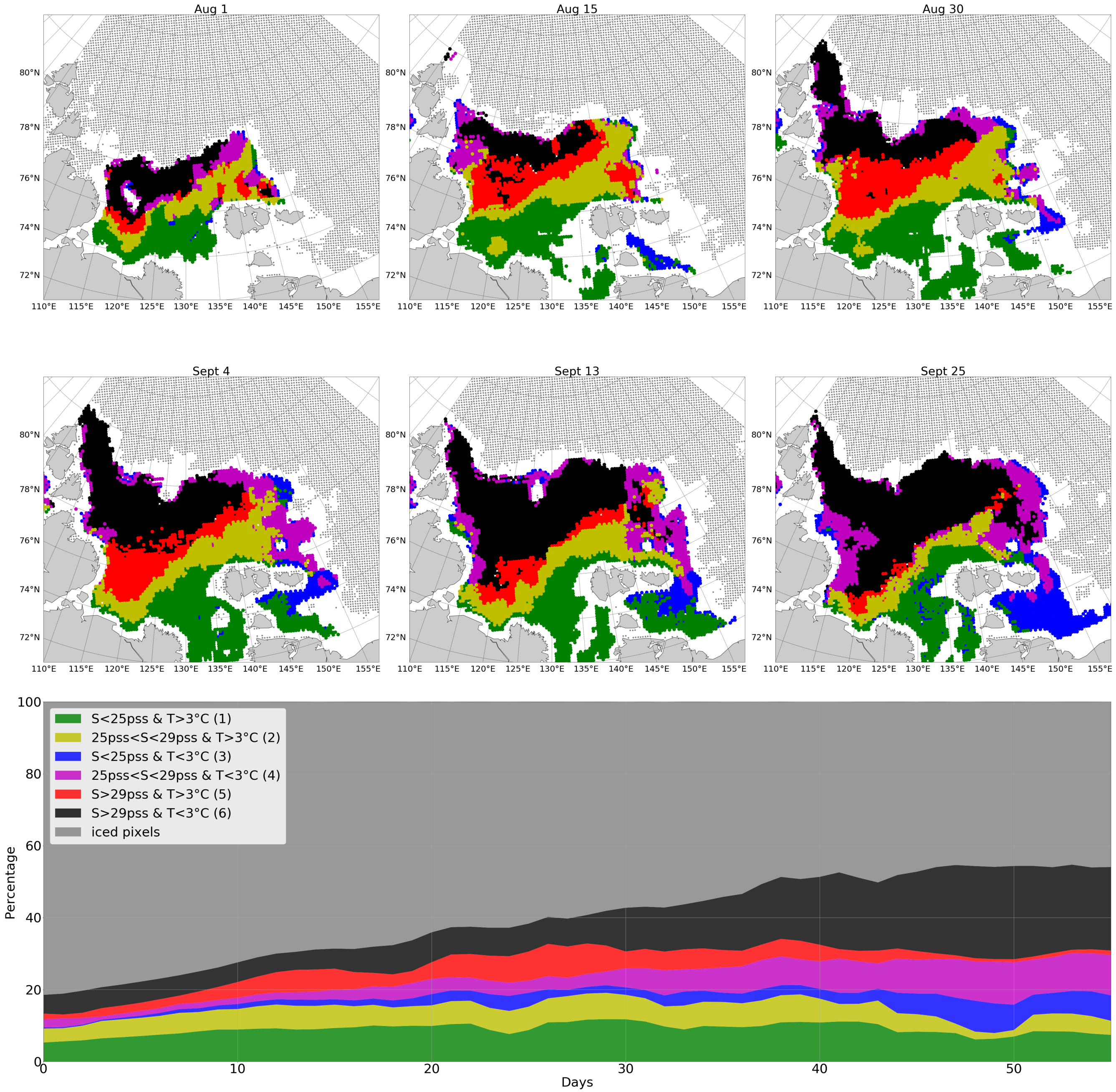

Figure 9. Spatial distribution of surface water masses in August-September 2018: upper row - Aug 1, Aug 15, Aug 30; lower row - Sept 4, Sept 13, Sept 30. Sea ice cover from AMSR2 is plotted as dashed area. The lowest panel show temporal evolution of surfaces occupied by each water mass or sea ice cover in the Laptev Sea (in % of the Laptev Sea surface).

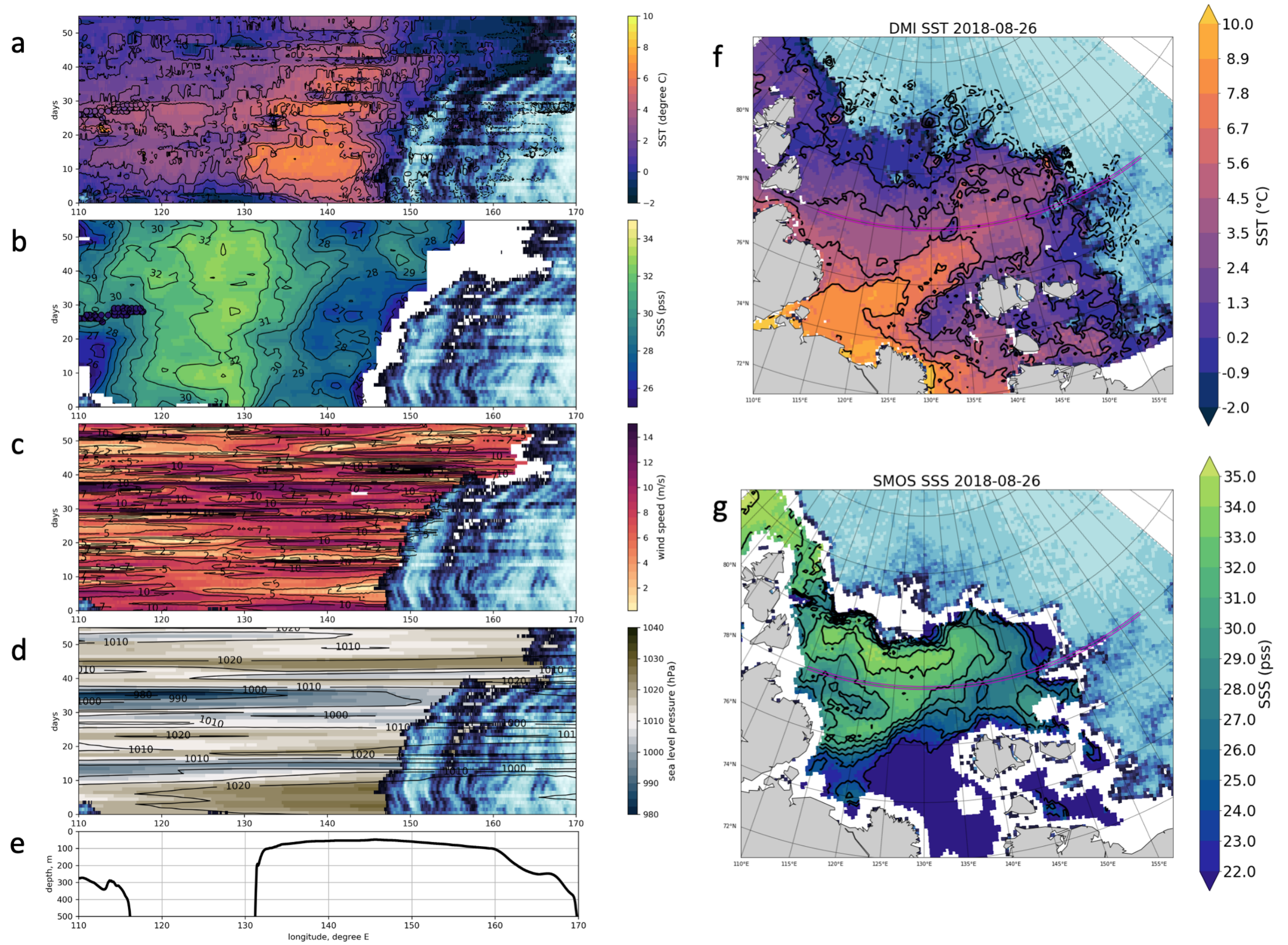

Figure 10. Hovmöller diagram of DMI SST (a), SMOS SSS "A" (b), ASCAT wind speed (c), and ERA5 sea level pressure (d) for the zonal transect at 78°N. Small coloured circles at SST and SSS diagrams show in situ measurements of temperature and salinity (first CTD or TSG at 6.5 m). Sea ice concentration (AMSR2) is indicated with a blue color, see Fig.5 for the color scale. The bathymetry along the virtual transect (e) is extracted from "1 Arc-Minute Global Relief Model" (**?**). The position of a virtual transect is shown at SST SMI and SMOS SSS "A" maps for August 26, 2018 (f, g).

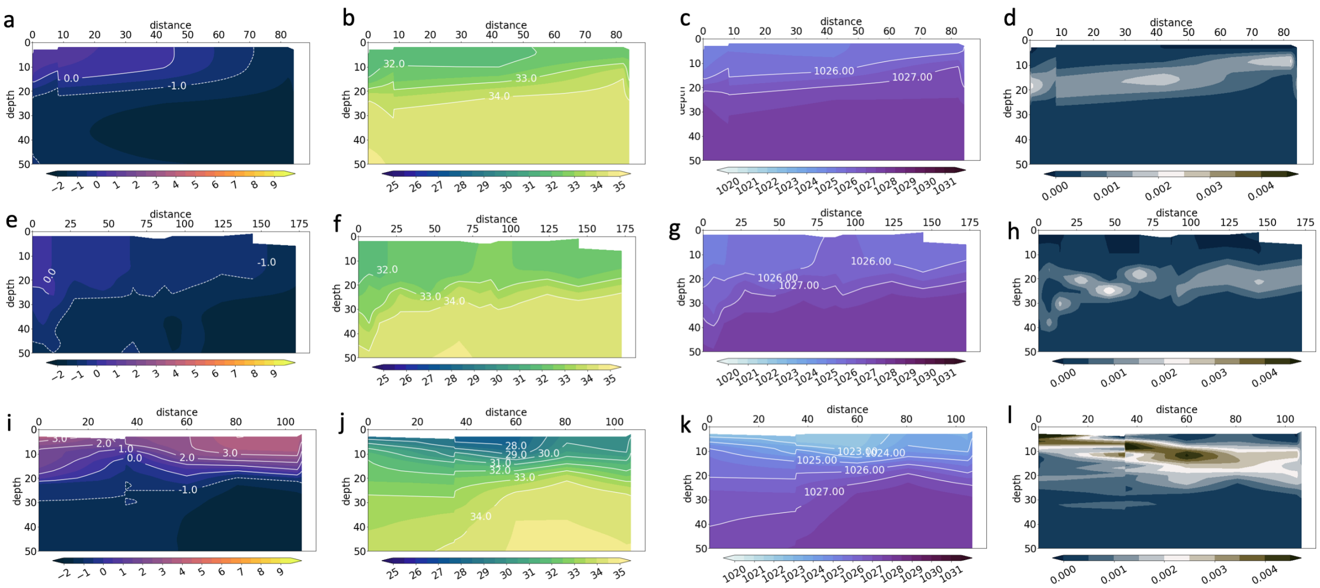

Figure 11. Temperature, °C, (left, first column), salinity, (second column), water density, kg/m^3 (third column) and buoyancy frequency, s^{-1}, (right, forth column) obtained from CTD measurements in the upper 50 m for section 1 northward of Arkticheskiy Cape (upper row), section 10 across the Shokalskiy Strait (second row), and section 4 across the Vilkitskiy Strait (lower row). See Fig.1 for the section's positions. The zero km is always placed at the southern point of each section

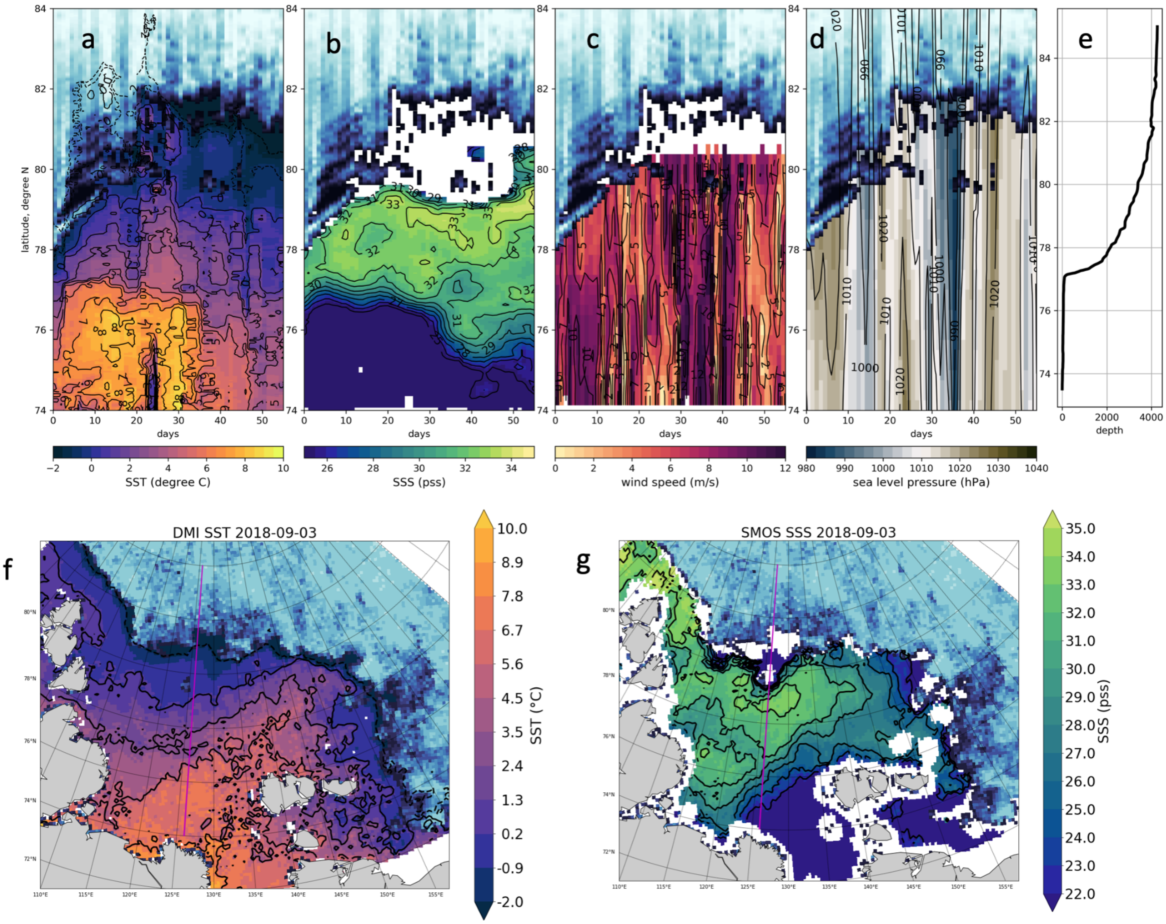

Figure 12. ~~Temperature, °C,~~ Hovmöller diagram of DMI SST (~~left, first column~~a), ~~salinity, PSS,~~ SMOS SSS "A" (~~second column~~b), ~~water density, kg/m^3~~ ASCAT wind speed (~~third column~~c) and ~~buoyancy frequency, $1/s$,~~ ERA5 SLP (~~right, forth column~~d) ~~obtained from CTD measurements in the upper 50 m~~ for ~~section 1 northward of Arkticheskiy Cape (upper row), section 10 across~~ the ~~Shokalskiy Strait~~ virtual meridional transect at 126°E. Sea ice concentration (~~second row~~AMSR2) is indicated with a blue color, ~~and section 4 across the Vilkitskiy Strait (lower row). See~~ see Fig.~~1~~ 5 for the ~~section's positions~~color scale. The ~~zero km is always placed at~~ bathymetry along the ~~southern point~~ transect (e) is extracted from "1 Arc-Minute Global Relief Model" (**?**. The position of ~~each section~~a virtual transect is shown on SST SMI and SMOS SSS "A" maps for August 26, 2018 (f, g).

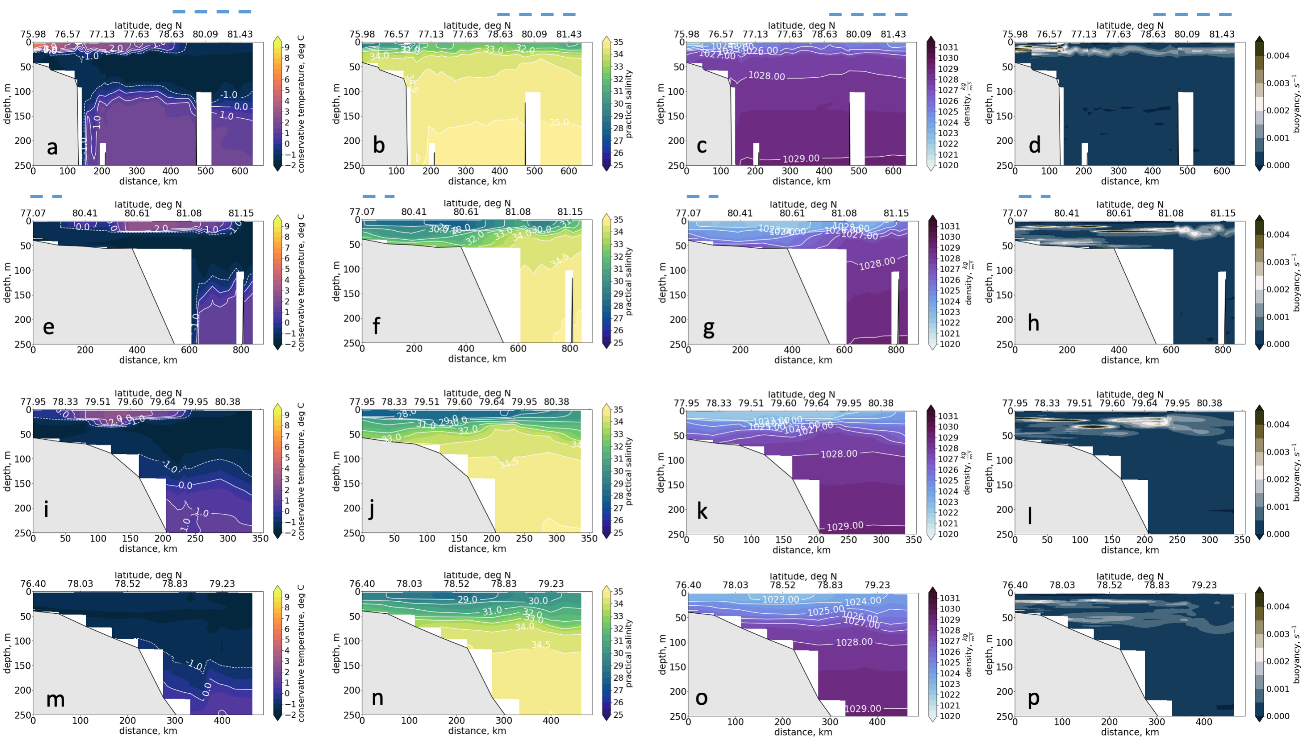

Figure 13. ~~Hovmöller diagram of SST~~Conservative temperature (left, ~~SSS~~first column), practical salinity (second column), density (third column) and ~~wind speed~~ Brünt-Vaisälä frequency (right, last column) in the upper 250 m along oceanographic section 5 (a-d); section 6 (e-h); section 8 (i-l); and section 7 (m-p). See Fig.1 for the ~~meridional transect at 126E~~section positions. ~~Sea ice concentration~~ The zero km is ~~indicated with~~ always placed at the southern point of each section. The dashed blue ~~color, see Fig~~line indicates the MIZ for sections 5 and 6 (the rest is ice-free area); the section 7 and 8 were done under the ice in MIZ.~~5~~

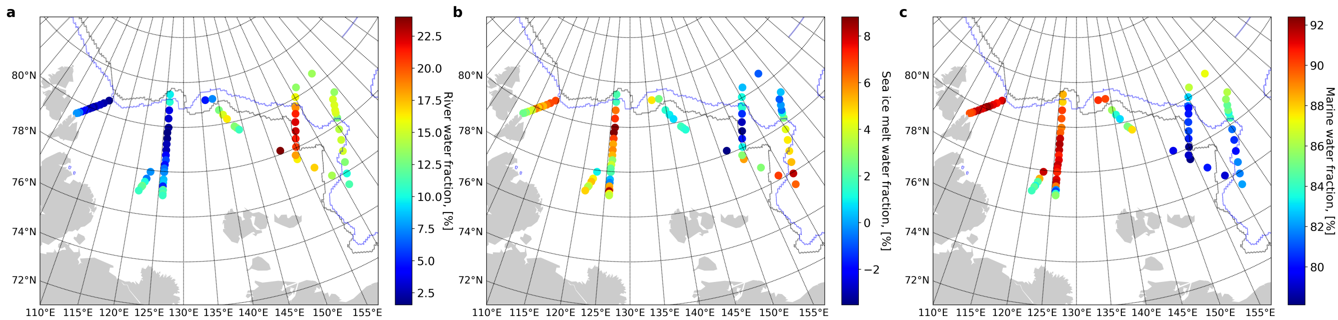

Figure 14. ~~Conservative temperature~~ Fractions of river water (~~left, first column~~a), ~~absolute salinity~~ sea ice melt water (~~second column~~b) ~~,~~ ~~density~~ and marine water (~~third column~~c), calculated using d-O18 measurements and ~~Brünt-Vaisälä frequency (right~~**?** 3-components model of freshwater balance. A thin black line shows the position of sea ice edge on August 31, ~~last column) in~~ 2018, when the ~~upper 250 m along oceanographic section 5~~ northern stations of the meridional (~~upper row~~5) ~~;~~ section ~~6 (second row); section 8 (third row);~~ along 126°E were done in the MIZ, and ~~section 7 (lower row). See Fig.1 for~~ the ~~section positions (~~blue line shows the ~~zero km is always placed at~~ sea ice edge on September 16, 2020, when the ~~southern point~~ ARKTIKA-2018 expedition was working in the MIZ of the East-Siberian Sea. Please, note that the colorbar scale is different for each ~~section)~~water fraction.

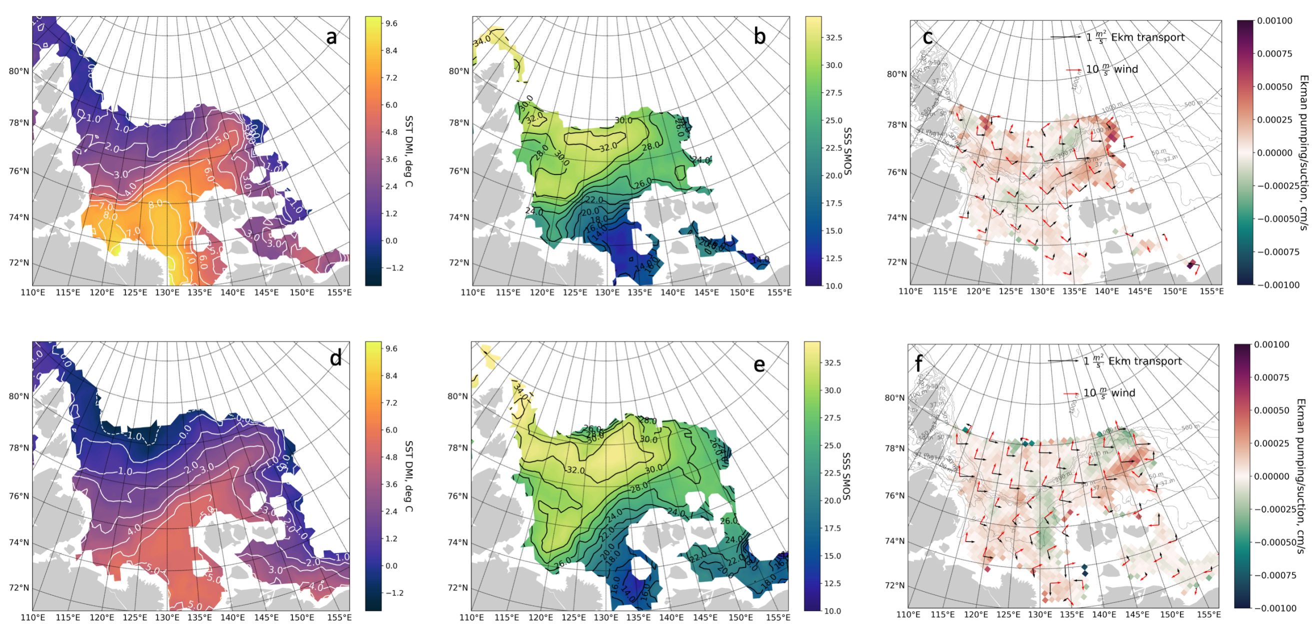

Figure 15. Mean monthly averages for August (upper row) and September (lower row): (a, d) SST, (b, e) SSS, (c, f) wind speed and direction ~~; (d-e)~~ shown with red arrows, horizontal ~~and vertical~~ Ekman transport with black arrows, Ekman vertical velocity (in cm/s) with color

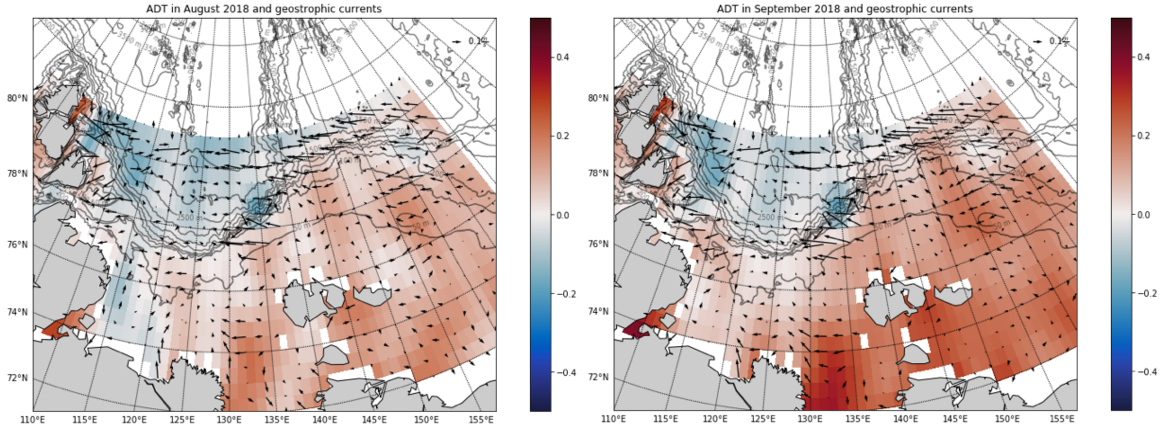

Figure A1. Absolute dynamic topography, cm and geostrophic currents, cm/s, in August and September 2018, calculated from DTU monthly Sea Level anomaly